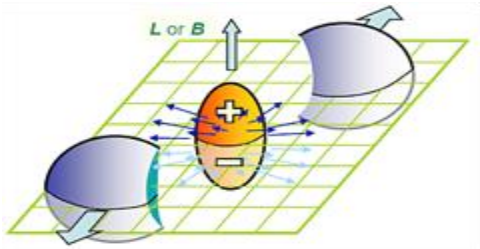
Strongly interacting QCD matter under extreme conditions

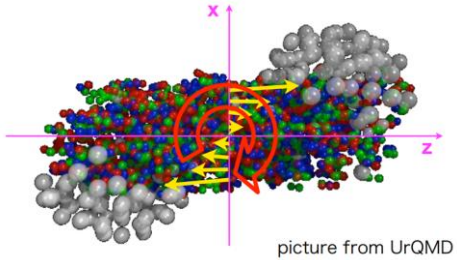
Defu Hou

Central China Normal University

Workshop on QCD Critical End Point and Effective Field Theory Methods 2026

QCD under new extreme conditions



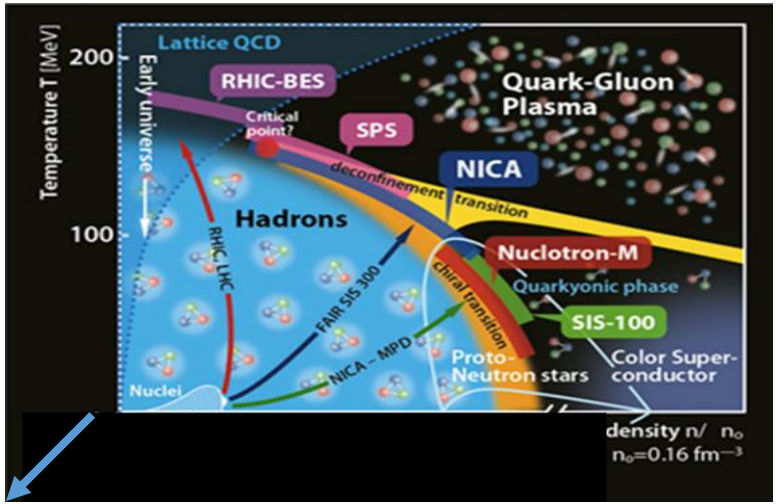




$$E, B \sim \gamma \frac{Z\alpha_{EM}}{R_A^2} \sim 3m_\pi^2$$

$$L \approx \frac{A\sqrt{s_{NN}}}{2} b\hbar \sim 10^6 \hbar$$

Explore the new dimensions of the QCD phase diagram



B, ω

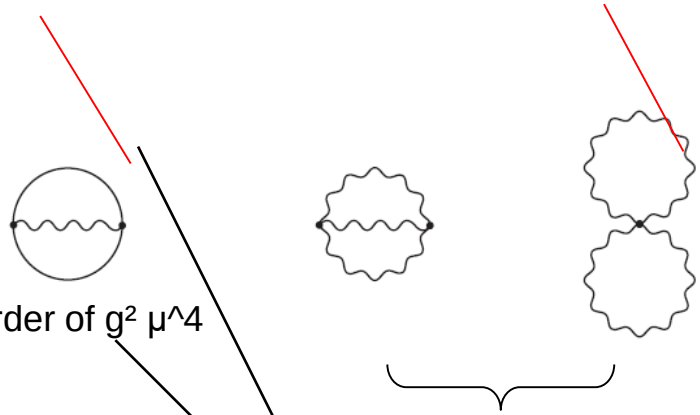
Outline

- **Introduction and motivation**
- **Phase structure under rotation and Magnetic field**
- **Transport properties of rotating magnetized matter**
- **Summary**

CJT effective action of QCD

$$\Gamma[\bar{D},\bar{S}] = \frac{1}{2}\{Tr\ln\bar{D}^{-1} + Tr(D^{-1}\bar{D} - 1) - Tr\ln\bar{S}^{-1} - Tr(S^{-1}\bar{S}) - 2\Gamma_2[\bar{D},\bar{S}]$$

2-loop approximation



Order of g² μ^4

Powers of T

Stationary points

$$\left.\frac{\delta\Gamma}{\delta\bar{\mathcal{D}}}\right|_{\mathcal{D}=\mathcal{D},\mathcal{S}=\mathcal{S}} = 0\,, \qquad \left.\frac{\delta\Gamma}{\delta\bar{\mathcal{S}}}\right|_{\mathcal{D}=\mathcal{D},\mathcal{S}=\mathcal{S}} = 0$$

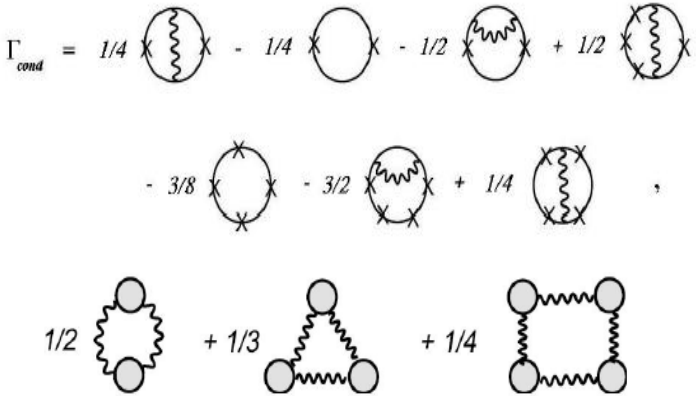
$$\mathcal{D}^{-1} = D^{-1} + \Pi[\mathcal{S}] \qquad \mathcal{S}^{-1} = \mathcal{S}_0^{-1} + \Sigma$$

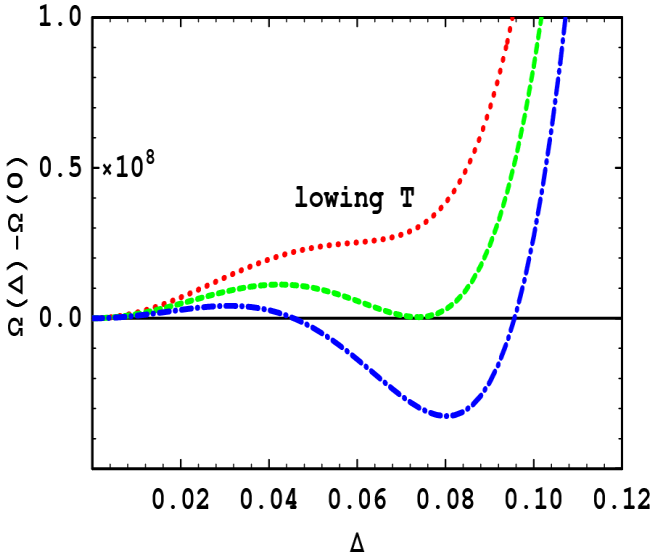
$$\Gamma_2[\bar{\mathcal{D}},\bar{\mathcal{S}}] = -\frac{1}{2}\mathrm{Tr}\{\bar{\mathcal{D}}\,\Pi[\bar{\mathcal{S}}]\}$$

D. Rischke Prog. Part. Nucl. Phys. 52 197 (2004)

Gauge field fluc. induce 1st order PT of CSC in dense QCD

Giannakis, Hou, Ren, Rischke, PRL 93 (2004); PRD 73 (2006)





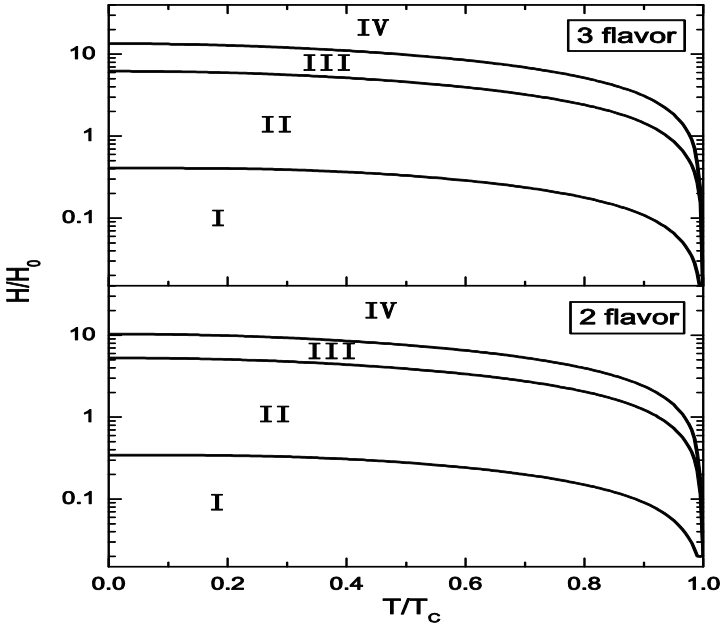
Introduction of $t\Delta^3 n$ in free energy by flucts. Inducing 1st order PT instead of 2nd order PT in MFA

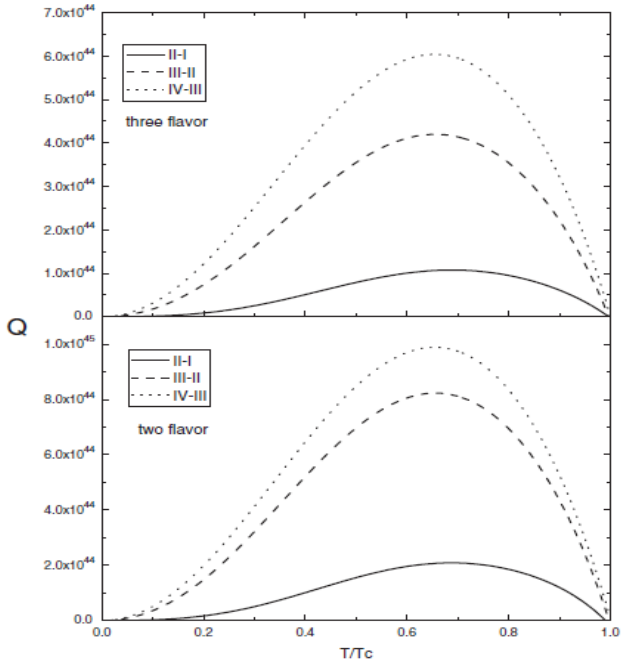
D. Rischke Prog. Part. Nucl. Phys. 52 197 (2004)

Nonspherical states in dense QCD with B

H0=5.44×10^14 G, 1.97×10^14 G

	I	II	III	IV	$T_C(10^{-1}$ MeV)
Two-flavor	CSL_u, CSL_d	$(polar)_u$, $(planar)_d$	$(normal)_u$, $(polar)_d$	$(normal)_u$, $(normal)_d$	1.35
Three-flavor	CSL_u, $CSL_{d,s}$	$(polar)_u$, $(planar)_{d,s}$	$(normal)_u$, $(polar)_{d,s}$	$(normal)_u$, $(normal)_{d,s}$	0.49



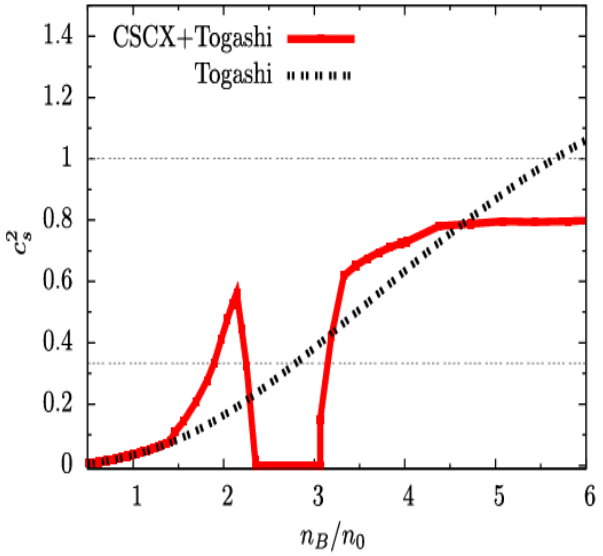


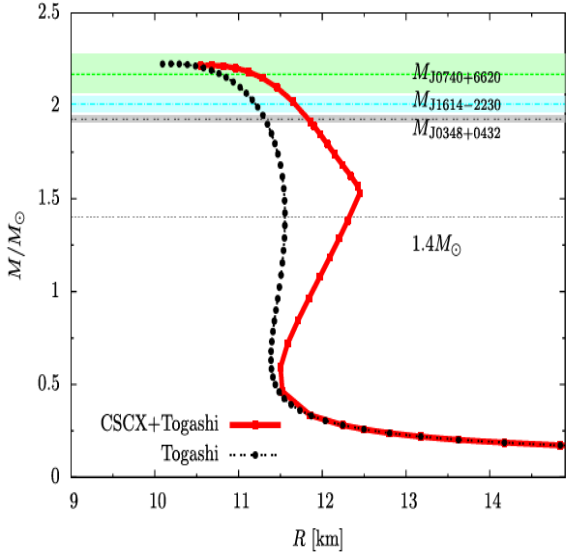
Feng, Hou, Ren,Wu, PRL 105(2010)

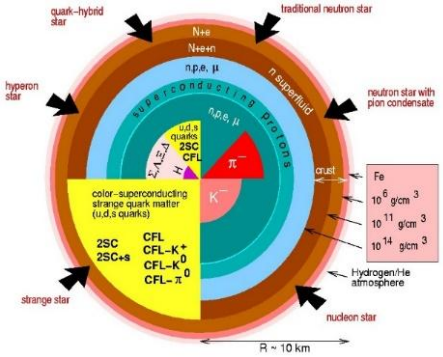
Wu, He, Hou, Ren, PRD84 (2011)

EoS of dense QCD matter and NSs

T. Kojo, D. F. Hou, Okafor, Togashi, PRD 104 (2021) 063036

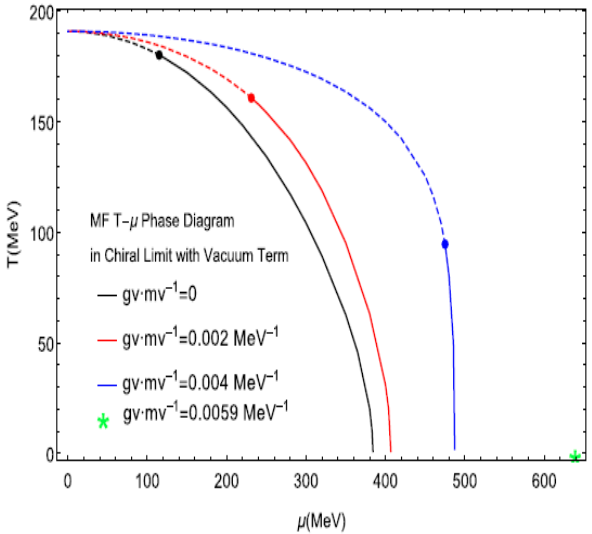


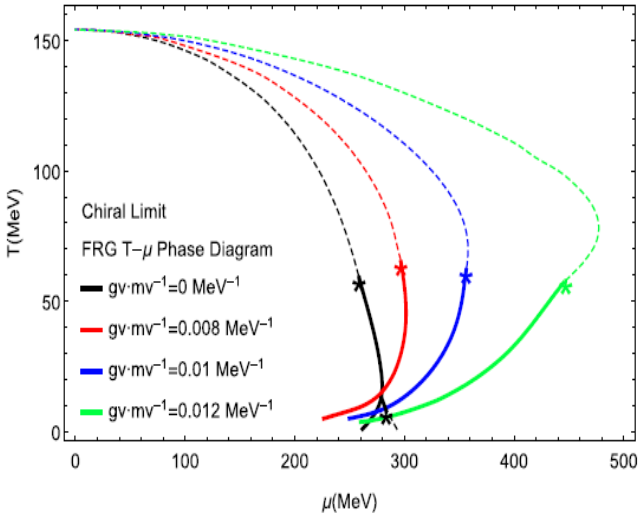




FRGE study of the phase diagram: fluctuations on the CEP

Zhang, Hou , Kojo, Qin, PRD96 (2017)

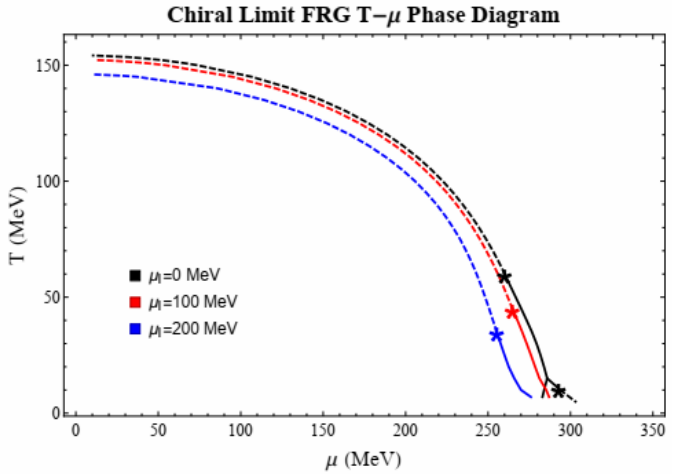


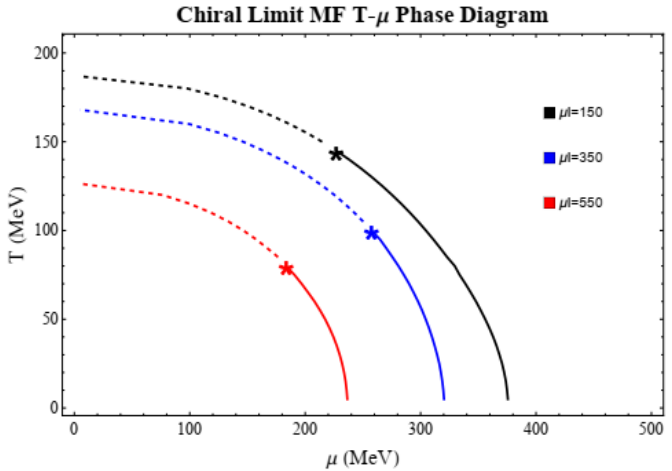


Nematic–isotropic (NI) puzzle with FRGE

Qin, Hou, Huang, Li, Zhang, PRB98, (2018)

Osman， Hou, Wang， Zhang， EPJC（2025）





- FRG:
  - **Sensitive to isospin chemical potential** μ_I and vector meson interactions.
  - Inclusion of μ_I and ρ meson **suppresses back-bending**.
  - Tricritical point (TCP) shifts to lower temperature and chemical potential.
  - Shows **weaker first-order transitions** and smoother crossovers at larger μ_I.
- MF: As μ_I increases, the TCP moves to **lower temperature** and **lower quark chemical**

Phase Structure of hQCD with magnetic field

The Einstein–Maxwell–dilaton (EMD) action*:

$$S=-\frac{1}{16\pi G_5}\int d^5x\sqrt{-g}[R-\frac{f_1(\phi)}{4}F_{(1)MN}F^{MN}-\frac{f_2(\phi)}{4}F_{(2)MN}F^{MN}-\frac{1}{2}\partial_M\phi\partial^M\phi-V(\phi)],$$

chemical potential　　B field　　breaking conformal sym.

The metric:

$$ds^2=\frac{L^2e^{S(z)}}{z^2}[-g(z)dt^2+dx_1^2+e^{B^2z^2}(dx_2^2+dx_3^2)+\frac{dz^2}{g(z)}],$$

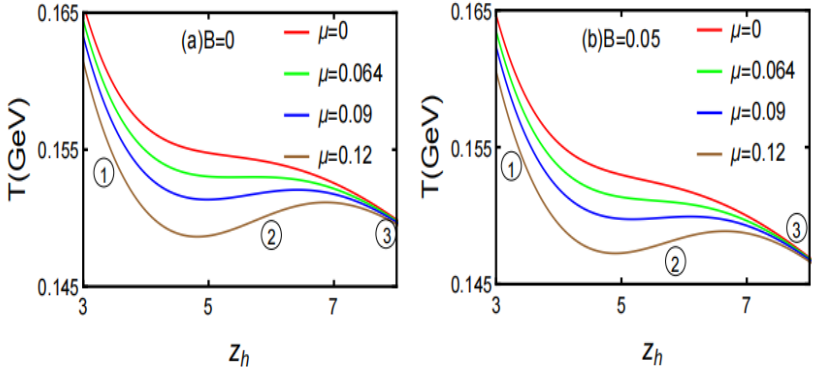
$$A_t(z)=\mu[1-\frac{\int_0^z d\xi\frac{\xi e^{-B^2\xi^2}}{f_1(\xi)\sqrt{S(\xi)}}}{\int_0^{z_h}d\xi\frac{\xi e^{-B^2\xi^2}}{f_1(\xi)\sqrt{S(\xi)}}}]=\widetilde{\mu}\int_z^{z_h}d\xi\frac{\xi e^{-B^2\xi^2}}{f_1(\xi)\sqrt{S(\xi)}},$$

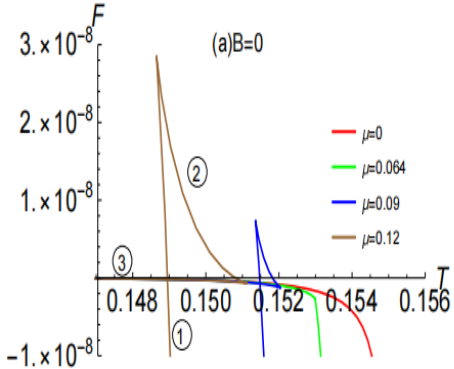
Dilaton field :

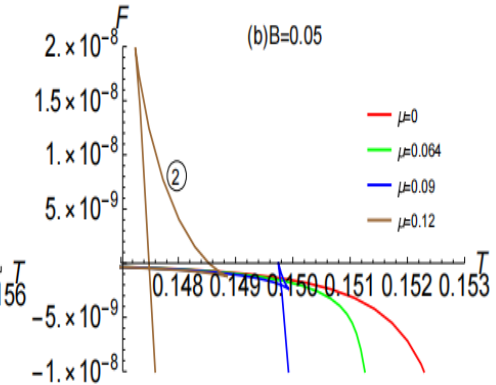
$$\phi(z)=\int dz\sqrt{-\frac{2}{z}(3zA''(z)-3zA'(z)^2+6A'(z)+2B^4z^3+2B^2z)}+K_5.$$

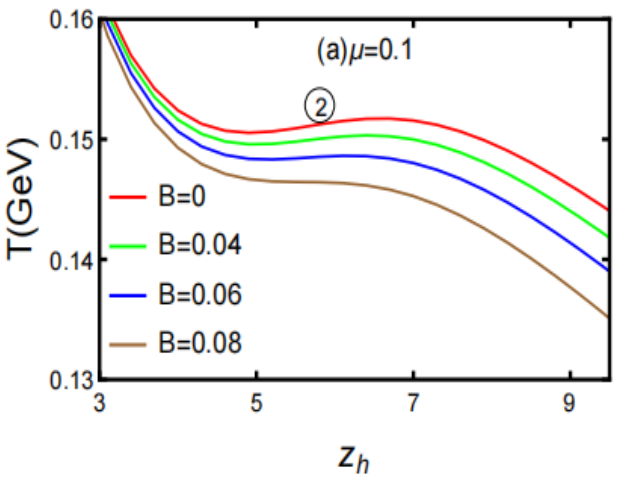
*Hardik Bohra a, David Dudal et al, Anisotropic string tensions and IMC from a dynamical AdS/QCD model.PLB 801 (2020) 135184.

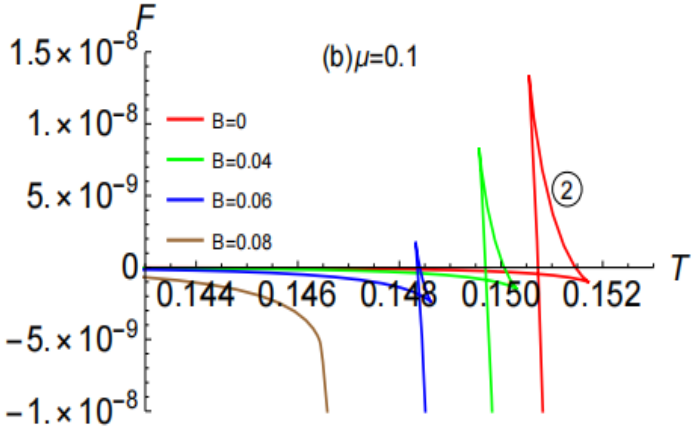
BH thermodynamics and hQCD with B





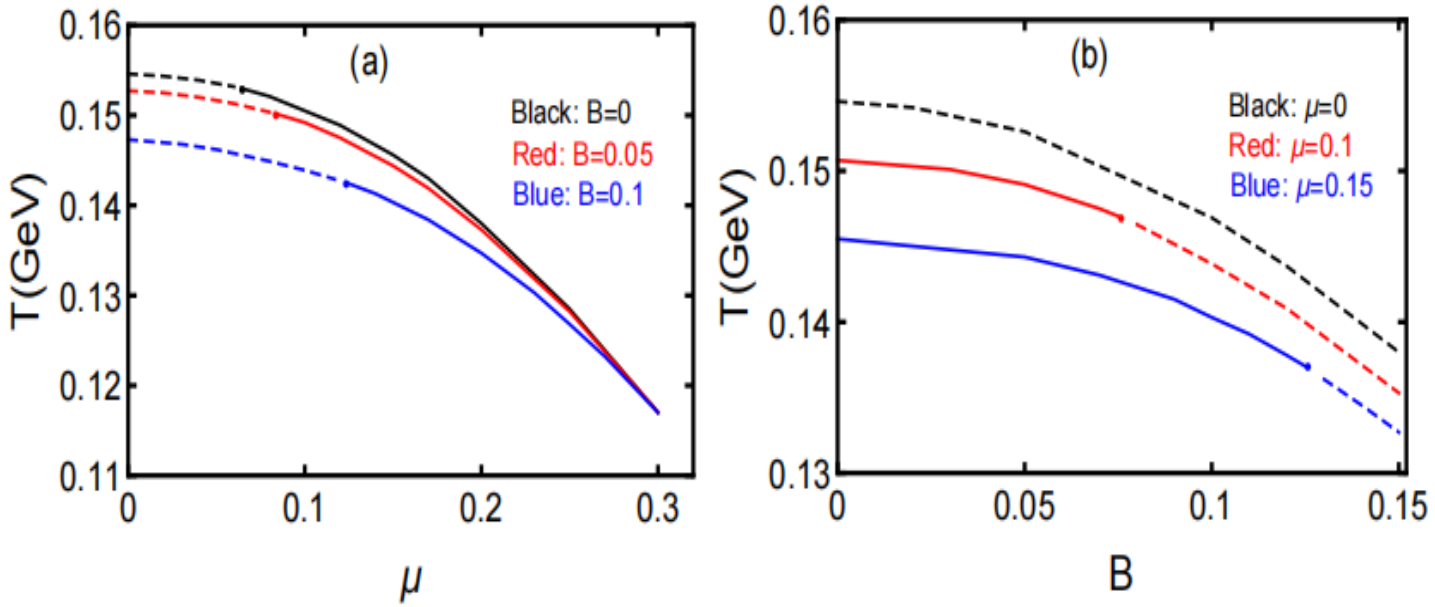






Z.-R. Zhu, D.-F. Hou, Inverse magnetic catalysis and energy loss in holographic QCD model, Phys. Rev. D 110 (2024) 066010

Phase diagram of hQCD with B



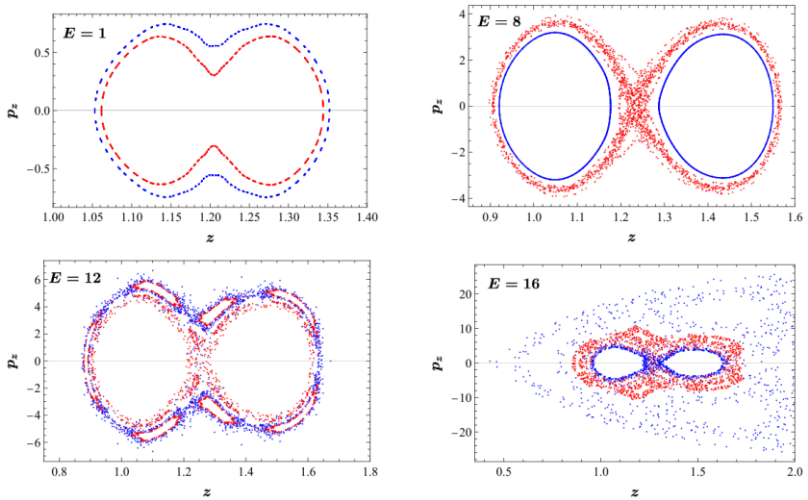
1) μ promotes the smooth crossover to first-order PT; B promotes the first-order PT to a crossover

2) Inverse magnetic catalysis

Z.-R. Zhu, D.-F. Hou, Phys. Rev. D 110 (2024) 066010

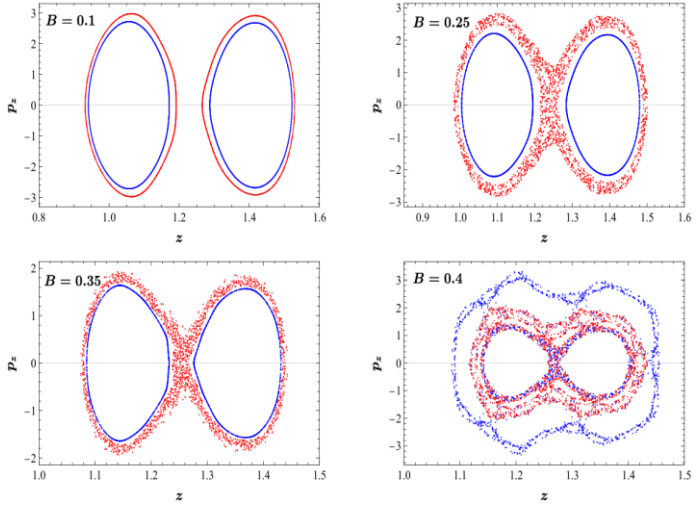
Chaos in the near-horizon dynamics of the dyonic AdS_4 - Reissner - Nordström black hole

The influence of **energy** on the **Poincar ésection**: $(z_h = 2)$



As E increases, the trajectory approaches the horizon, KAM tori distort and twist, and ultimately break up and vanish, replaced by progressively larger and more complex chaotic layers (scattered-point regions).

M. Y. Wang, Y. Q. Zhao, S. W. Li, Hou, D. Yan
JHEP 07 (2026) 040



B field leads to the progressive breakup of KAM tori and the expansion of chaotic layers, the origin of chaos can be not only the BH horizon, but also strong external fields.

Phase diagram @2+1 flavor

- **Holographic model:** *[1]. R.-G. Cai, S. He, L. Li and Y.-X. Wang, Phys. Rev. D 106 (2022) L121902*
  - **The action:**

$$S_M = \frac{1}{2\kappa_N^2}\int d^5x\sqrt{-g}[\mathcal{R} - \frac{1}{2}\nabla_\mu\phi\nabla^\mu\phi - \frac{Z(\phi)}{4}F_{\mu\nu}F^{\mu\nu} - V(\phi)],$$

where the potential and kinetic functions read

$$V(\phi) = -12\cosh[c_1\phi] + \left(6c_1^2 - \frac{3}{2}\right)\phi^2 + c_2\phi^6,$$

Capturing the behavior of EOS at zero chemical potential.

$$Z(\phi) = \frac{1}{1+c_3}sech[c_4\phi^3] + \frac{c_3}{1+c_3}e^{-c_5\phi}.$$

Capturing the flavor dynamic.

  - **The metric:**

$$ds^2 = -e^{-\eta(r)}f(r)dt^2 + \frac{dr^2}{f(r)} + r^2(dx_1^2 + dx_2^2 + dx_3^2),$$
$$\phi = \phi(r), \qquad A_t = A_t(r),$$

- **The Hawking temperature and entropy density:**

$$T = \frac{1}{4\pi}f'(r_h)e^{-\eta(r_h)/2} \qquad s = \frac{2\pi}{\kappa_N^2}r_h^3.$$

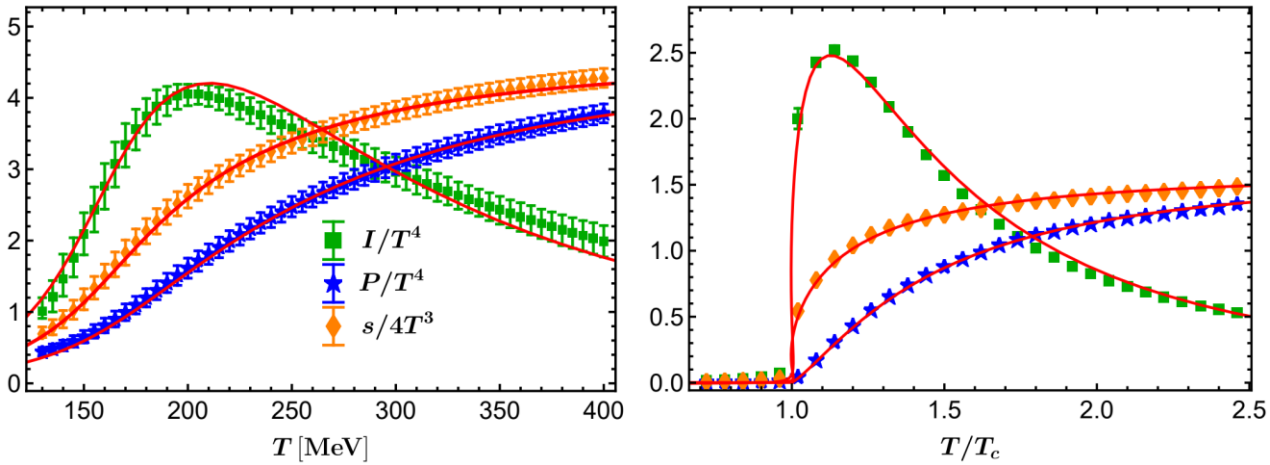
effective Newton constant

The parameter:

model	c_1	c_2	c_3	c_4	c_5	κ_N^2	ϕ_s(GeV)	b
pure $SU(3)$	0.735	0				$2\pi(4.88)$	1.523	-0.36458
2 flavor	0.710	0.0002	0.530	0.085	30	$2\pi(3.72)$	1.227	-0.25707
2+1 flavor	0.710	0.0037	1.935	0.085	30	$2\pi(1.68)$	1.085	-0.27341

[1]. R.-G. Cai, S. He, L. Li and Y.-X. Wang, Phys. Rev. D 106 (2022) L121902

[2]. Y.-Q. Zhao, S. He, D. Hou, L. Li and Z. Li, , [2310.13432].



Lattice

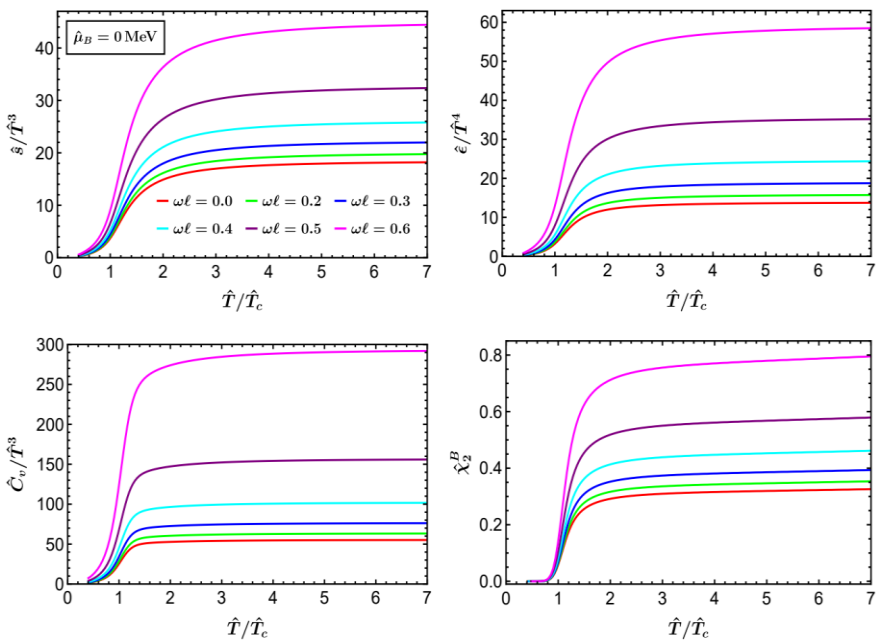
[3]. Phys.Rev.D 90 (2014) 094503
•e-Print: 1407.6387

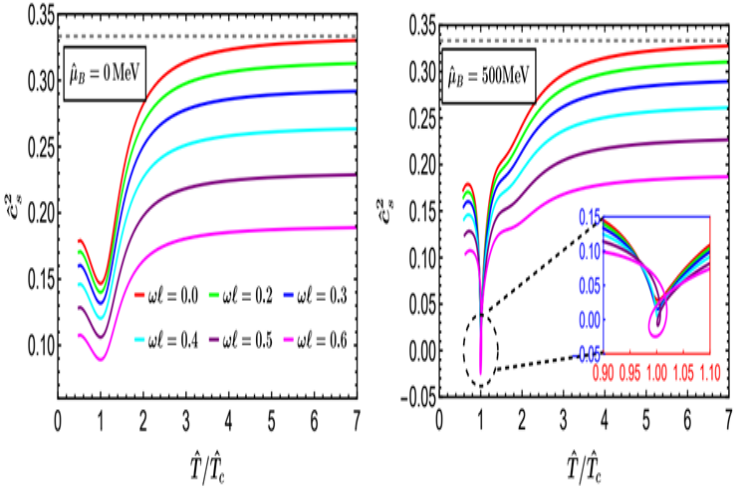
[4]. Phys.Rev.D 98 (2018) 5, 054513
• e-Print: 1801.03110

[5]. S. He, L. Li, Z. Li and S. Wang, [arXiv:2210.14094]

Phase diagram @2+1 flavor

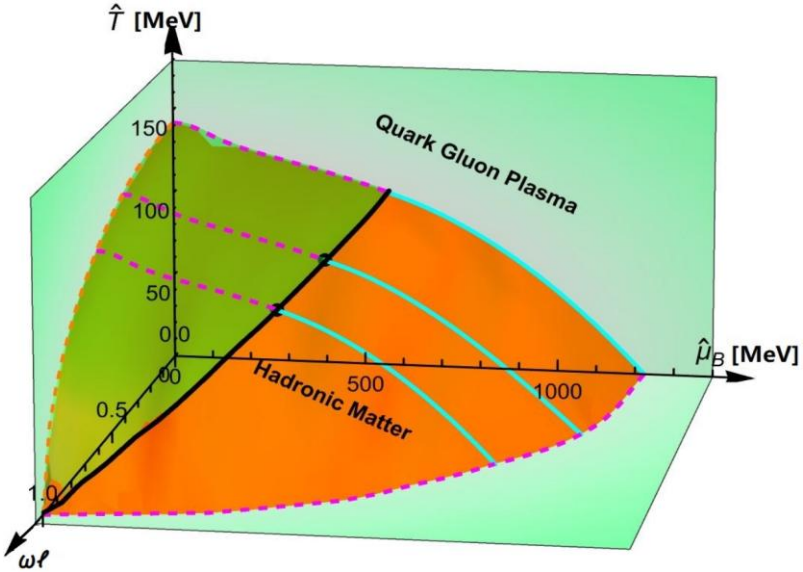
- Thermodynamics *with rotation*:

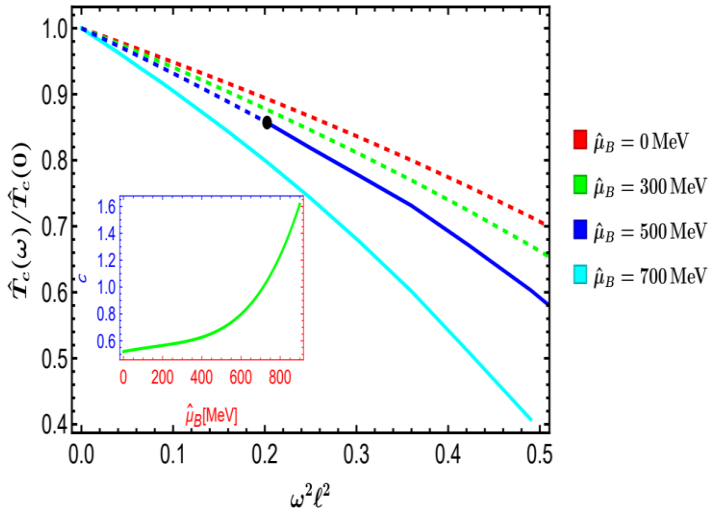




Yan-Qing Zhao, Song He, Defu Hou, Li Li, Zhibin Li, JHEP 04 (2023) 115 • e-Print: 2212.14662

QCD Phase structure with rotation for 2+1 flavors :





- ✓ **black solid line:** denoting the location of CEP.
- ✓ At high $\hat{T}$and small $\hat{\mu}_B$: **Being the smooth crossover.**
- ✓ At low $\hat{T}$and large $\hat{\mu}_B$: **Being 1st-order transition.**

YQ Zhao, S He , Hou, Li , Li, JHEP04 (2023)115

Chen, , Zhang, Li, Hou M.Huang , JHEP 07 (2021) 132

Lattice: Phys.Rev.D 103 (2021) 9, 094515,

Strong Coupling Expansion of Gluodynamics on a Lattice under Rotation

Gibbs free energy reads

$$\mathcal{F} = -T\ln\mathcal{Q} \qquad \mathcal{Q} = \mathrm{Tr}\exp[-\frac{1}{\mathrm{T}}(\mathrm{H}-\omega \mathrm{J_z})]$$

For a slow rotation, we have

$$\mathcal{F}[\mathcal{W},T] = \mathcal{F}^{(0)} - \frac{1}{2}I\omega^2 + O(\omega^4) = \mathcal{F}^{(0)} - \frac{v^2}{2R^2}I + O(\omega^4)$$

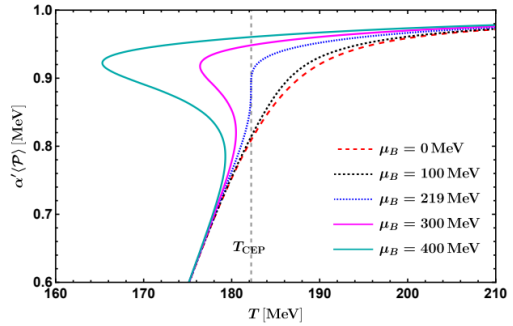
The transition temperature to the leading order correction by a small linear speed $v = \omega R$ at the boundary is given by

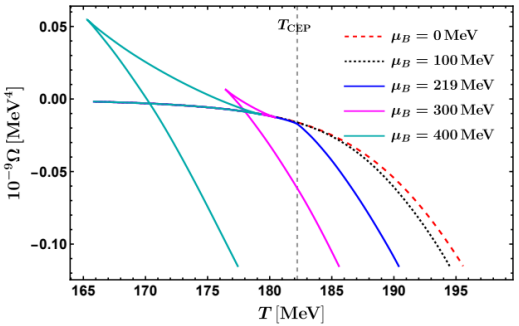
$$T_d = T_d^{(0)}(1 + Bv^2) \qquad \boldsymbol{B = -\frac{1}{24\sigma a^2} \approx -0.01119}$$

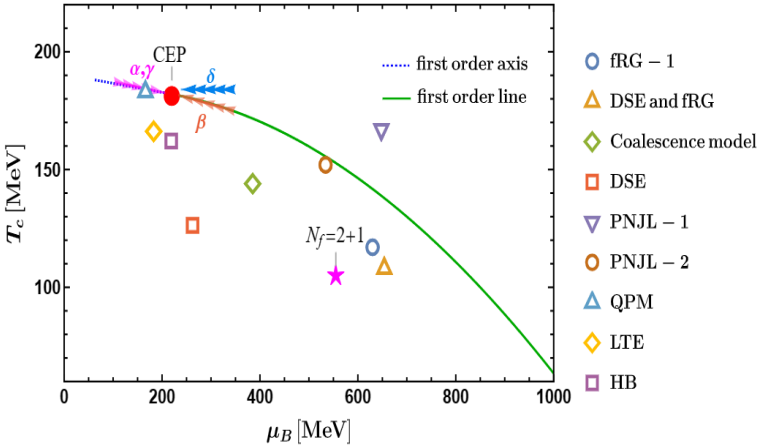
We find that the deconfinement T decreases with the angular velocity, opposite to the tendency revealed in lattice simulations but in line with most of holographic results.
We also find the string tension is enhanced by rotation.

S Chen, DF Hou, HC Ren， arXiv:2505.15487
K. Fukushima, Y. Shimada, arXiv: 2506.03560
JC Yang, XG Huang arXiv: 2307.5755
Braguta et. al. arXiv:2102.05084

Phase structure of 2 flavor







[2]. Y.-Q. Zhao, S. He, D. Hou, L. Li and Z. Li, [2310.13432], PRD (2024)

Critical behavior

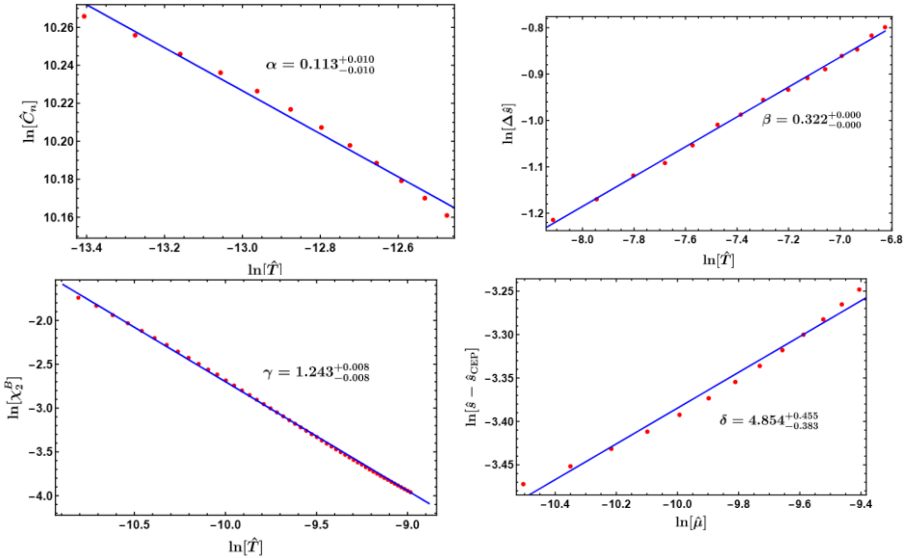
$$C_n \equiv T\left(\frac{\partial s}{\partial T}\right)_{n_B} \sim |T - T_{\rm CEP}|^{-\alpha}$$

$$\Delta s = s_> - s_< \sim (T_{\rm CEP} - T)^{\beta}.$$

$$\chi_2^B = \frac{1}{T^2}\left(\frac{\partial n_B}{\partial \mu_B}\right)_T \sim |T - T_{\rm CEP}|^{-\gamma}.$$

$$s - s_{\rm CEP} \sim |\mu_B - \mu_{\rm CEP}|^{1/\delta}$$

	Experiment	3D Ising	Mean field	DGR model	Ours
α	0.110-0.116	0.110(5)	0	0	$0.113^{+0.010}_{-0.010}$
β	0.316-0.327	0.325±0.0015	1/2	0.482	$0.322^{+0.000}_{-0.000}$
γ	1.23-1.25	1.2405±0.0015	1	0.942	$1.243^{+0.008}_{-0.008}$
δ	4.6-4.9	4.82(4)	3	3.035	$4.854^{+0.455}_{-0.383}$

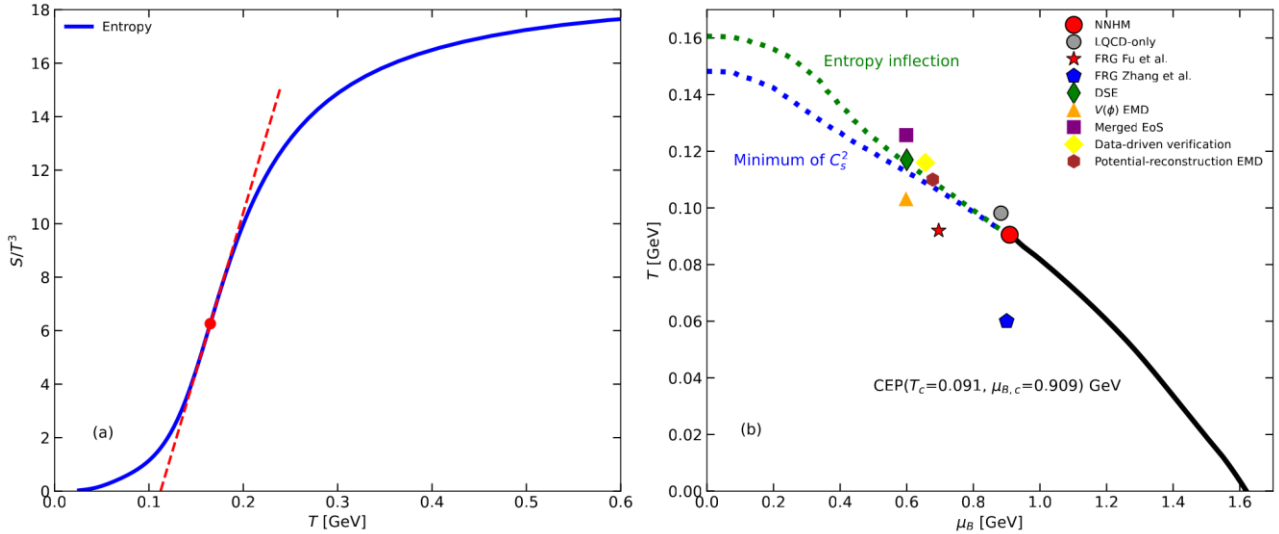


Yan-Qing Zhao, Song He, Defu Hou, Li Li, Zhibin Li （ Phys.Rev.D 109 (2024) 8, 086015 ）

Neural-Network Holographic Model of the QCD Phase Transition under Lattice and HRG Constraints

De-Xing Zhu, Li-Qiang Zhu, Xun Chen, De-Fu Hou, Kai Zhou, arXiv:2603.25571.

Localization of the CEP and Phase Structure :



QCD phase structure from the data-driven NNHM. (a) Pseudo-critical temperature determined from the inflection point of s/T^3. (b) QCD phase diagram in the $T-\mu$ plane.

NLO correction to the jet quenching parameter

Zhang, Hou, Ren, JHEP 01 (2013) 032

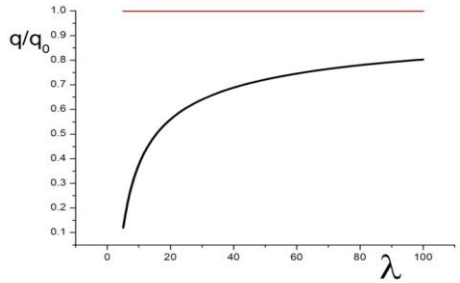
dominant

$$\hat{q} = \frac{\pi^{3/2}\Gamma(\frac{3}{4})}{\Gamma(\frac{5}{4})}\sqrt{\lambda}T^3[1-1.97\lambda^{-1/2}+O(\lambda^{-1})]$$

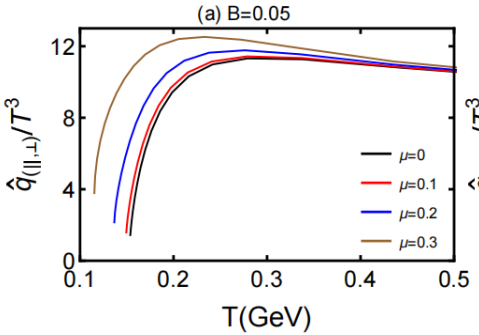
H. Liu, K. Rajagopal, and U. A. Wiedemann, Phys. Rev. Lett. 97, 182301 (2006).

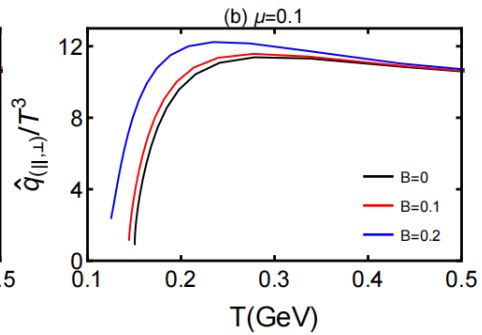
$$1 - 1.765\lambda^{-3/2}.$$

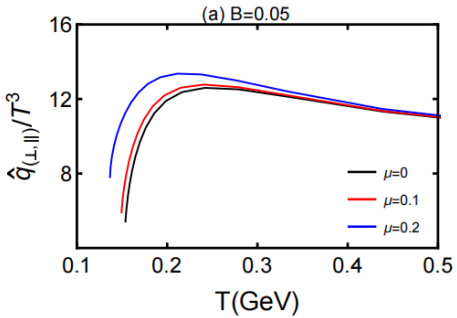
Armesto et al., JHEP 09 (2006)

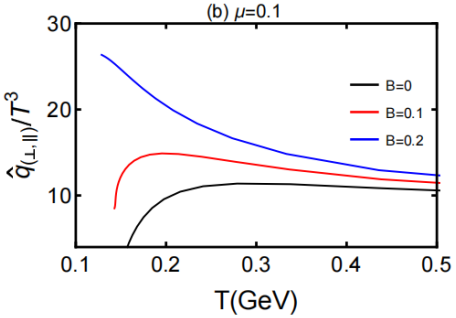


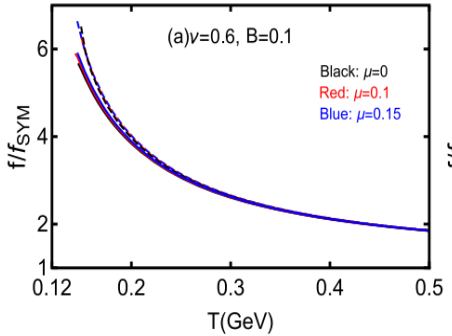
Jet quenching around Tc with B

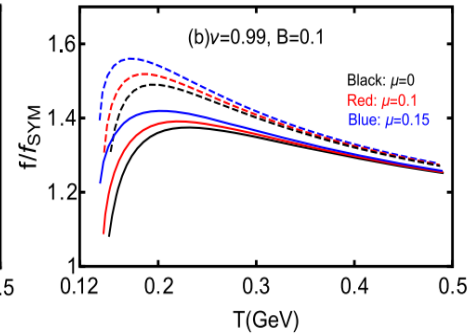












$\hat{q}_\perp > \hat{q}_\parallel$; μ、B enhance $\hat{q}$

$\hat{q}$ enhenced around T_c agrees with Laticce results(150-250MeV);

Z.-R. Zhu, D.-F. Hou, Phys. Rev. D 110 (2024) 066010 .

Drag force

J.X. Chen, DH, H.C Ren , JHEP03 (2024) 171 , arXiv: 2308.08126

Components of drag force

$$\frac{dp_\mu}{dt} = -\frac{1}{2\pi\alpha'}\frac{\partial \mathcal{L}}{\partial(\frac{\partial X^\mu}{\partial r})}$$

Drag force of μ component

Azimuthal $$\frac{dp_\phi}{dt} = -\frac{\pi\sqrt{\lambda}T^2}{2}\omega l_0^2\frac{1}{\sqrt{1-v^2}}$$

Radial $$\frac{dp_l}{dt} = -\omega^2 l_0\frac{1}{\sqrt{1-v^2}}\left[\frac{T\sqrt{\lambda}}{2(1-v^2)^{\frac{1}{4}}} - m_{rest}\right]$$

Centralfugal force, cut off $r_m = 2\pi\alpha' m_{res}$

Longitudinal $$\frac{dp_z}{dt} = -\frac{\pi\sqrt{\lambda}T^2}{2}\frac{v}{\sqrt{1-v^2}}\left(1+\frac{\omega^2 l_0^2}{2}\frac{1}{1-v^2}\right)$$

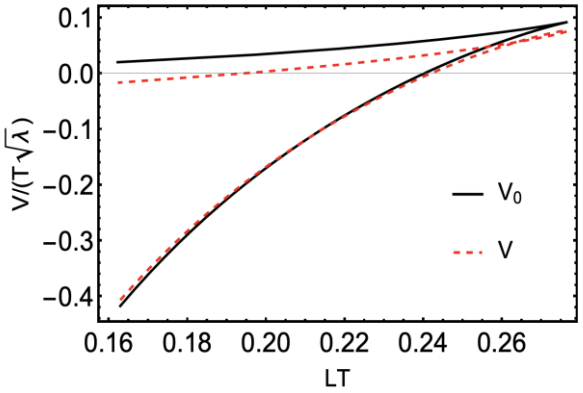
$\propto \omega^2$

$\omega = 0$ $\Longrightarrow$ $\frac{dp_\phi}{dt} = 0,$ $\frac{dp_l}{dt} = 0,$ $\frac{dp_z}{dt} = -\frac{\pi\sqrt{\lambda}T^2}{2}\frac{v}{\sqrt{1-v^2}}$

S. S. Gubser, PRD 74, 126005 (2006); C. P. Herzog et al., JHEP 07 (2006) 013

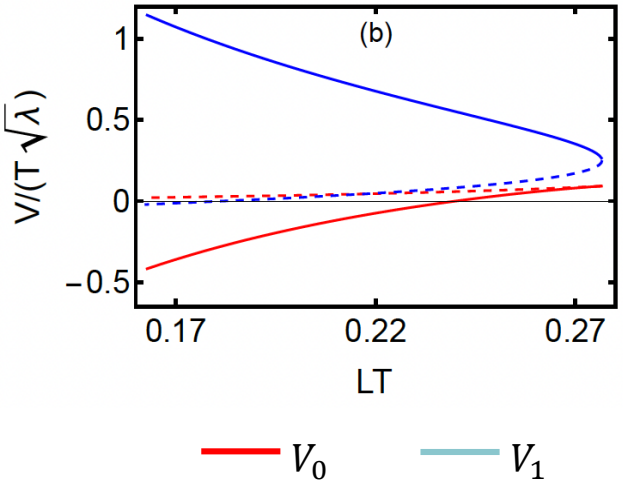
Heavy quark potential

$$V(L) = V_0(L) + \omega^2 l_0^2 V_1(L) + O(\omega^4)$$



1. Binding force ↓
2. Force range ↑

$$V(L) = V_0(L) + \frac{1}{4}\omega^2 L^2 V_1(L) + O(\omega^4)$$

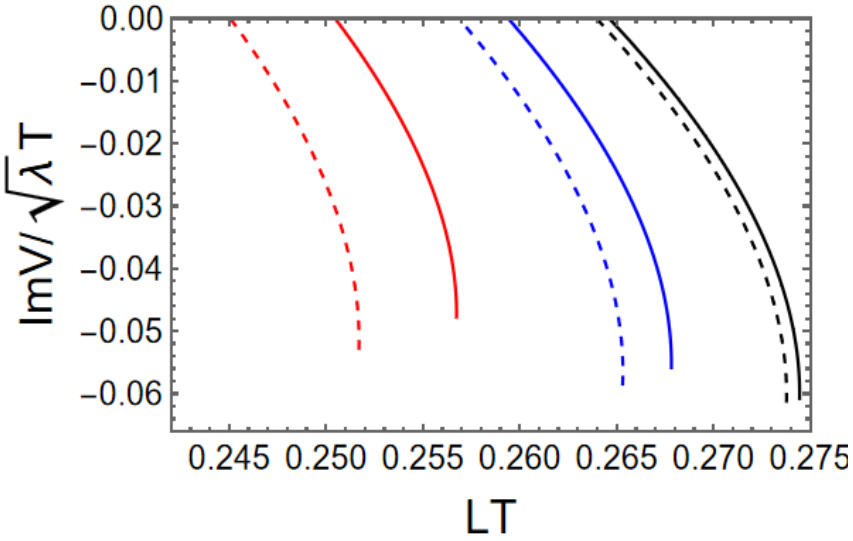


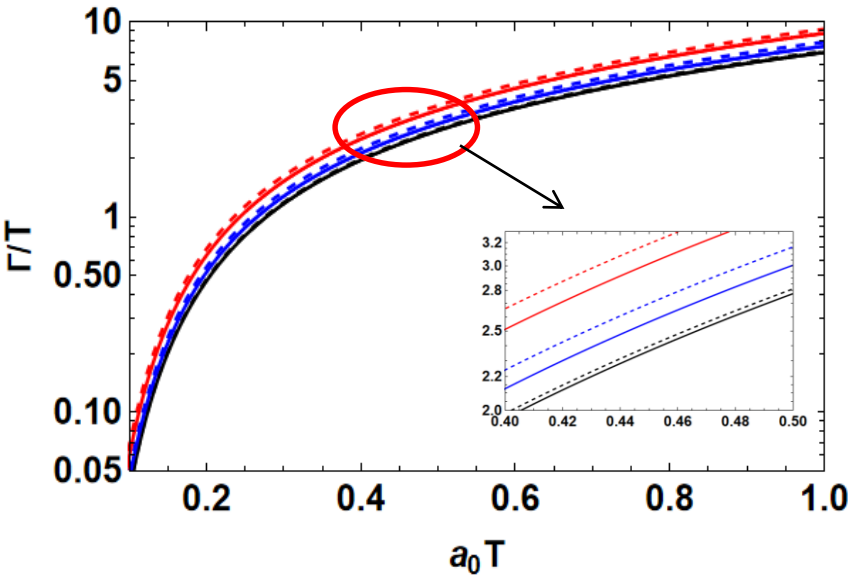
$V_\perp$

Potential ↑
Force range ↓

J. X. Chen, D. Hou, H. C. Ren, JHEP 03 (2024) 171

Imaginary potential and thermal width in a spinning black hole background





Our results reveal that increasing the boost parameter causes the imaginary potential to emerge at smaller interquark distances, suggesting that boost parameter accelerates quarkonium melting. Furthermore, we find that boost parameter enhances the thermal width

* Zhou-Run Zhu, Sheng Wang, Yang-Kang Liu,and Defu Hou. Phys. Rev. D 110 (2024) 126008

Spectral function and spin alignment
Heavy quarkonium

J/Ψ in the holographic model

- **Background model:**

H. Bohra et al., Phys. Lett. B 801 (2020) 135184

- **The Lagrangian :**

$$\mathcal{L} = \sqrt{-g}\Big(R - \frac{g_1(\phi_0)}{4} F_{(1)\mu\nu} F^{\mu\nu} - \frac{g_2(\phi_0)}{4} F_{(2)\mu\nu} F^{\mu\nu} - \frac{1}{2}\partial_\mu\phi_0\partial^\mu\phi_0 - V(\phi_0)\Big).$$

- **The metric ansatz:**

External magnetic field in x_1 direction.

B is the 5d magnetic field, in units GeV.

$$ds^2 = \frac{R^2 S(z)}{z^2}\Big(- f(z)dt^2 + dx_1^2 + e^{B^2 z^2}(dx_2^2 + dx_3^2) + \frac{dz^2}{f(z)}\Big),$$

$$\phi_0 = \phi_0(z), \quad A_{(1)\mu} = A_t(z)\delta^t_\mu, \quad F_{(2)} = B dx_2 \wedge dx_3,$$

$$f(z) = 1 + \int_0^z d\xi \xi^3 e^{-B^2\xi^2 - 3A(\xi)}\Big[K + \frac{\tilde{\mu}^2}{2R_{gg}R^2} e^{R_{gg}\xi^2}\Big],$$

$$K = -\frac{1 + \frac{\tilde{\mu}^2}{2R_{gg}R^2}\int_0^{z_h} d\xi \xi^3 e^{-B^2\xi^2 - 3A(\xi) + R_{gg}\xi^2}}{\int_0^{z_h} d\xi \xi^3 e^{-B^2\xi^2 - 3A(\xi)}},$$

$$\tilde{\mu} = \frac{\mu}{\int_0^{z_h} d\xi \frac{\xi e^{-B^2\xi^2}}{g_1(\xi)\sqrt{S(\xi)}}},$$

4d physical magnetic field is $e\mathcal{B} \sim \frac{const}{R} \times B$

$const = 1.6$

$$S(z) = e^{2A(z)}, \quad A(z) = -az^2$$

$a = 0.15\,\mathrm{GeV}^2$ Determined by matching with the lattice QCD deconfinement temperature at B = 0 GeV, Tc=0.268GeV

$R_{gg} = 1.16\,\mathrm{GeV}^2$ Determined by fitting the mass of J/Ψ

- **The Hawking temperature :**

$$T(z_h, \mu, B) = \frac{-z_h^3 e^{-3A(z_h) - B^2 z_h^2}}{4\pi}\Big(K + \frac{\tilde{\mu}^2}{2R_{gg}R^2} e^{R_{gg} z_h^2}\Big).$$

➢ Matter field model:

[2]. Phys. Lett. B 774, 476 (2017). arXiv:1709.05326

➢ **The standard Maxwell action :**

$$S = \int d^4x dz \sqrt{-g} e^{-\phi(z)} \left[-\frac{1}{4{g_5}^2} F_{mn} F^{mn} \right],$$

The scalar field $\phi(z)$, including three energy parameters, is used to parameterize different mesons,

$$\phi(z) = \kappa^2 z^2 + Mz + \tanh\left(\frac{1}{Mz} - \frac{\kappa}{\sqrt{\Gamma}}\right),$$

κ labels the quark mass,

Γ is the string tension of the quark pair

M denotes a large mass related to the heavy quarkonium non-hadronic decay.

$$\kappa_c = 1.2\,\text{GeV}, \quad \sqrt{\Gamma_c} = 0.55\,\text{GeV}, \quad M_c = 2.2\,\text{GeV},$$
$$\kappa_b = 2.45\,\text{GeV}, \quad \sqrt{\Gamma_b} = 1.55\,\text{GeV}, \quad M_b = 6.2\,\text{GeV}.$$

➢ **The spectral function is defined by the retarded Green's function:**

$$\rho(\omega) \equiv -ImG_R(\omega) = \omega Re\,\sigma|_{z=0}.$$

➢ **The equation of motion:**

$$\partial_m(\sqrt{-g} e^{-\phi(z)} F^{mn}) = 0.$$

➢ **The spectral function for vector meson will be calculated by membrane paradigm:**

[3] N. Iqbal, H. Liu, Phys. Rev. D 79, 025023 (2009). arXiv:0809.3808

- the conjugate momentum of the gauge field:

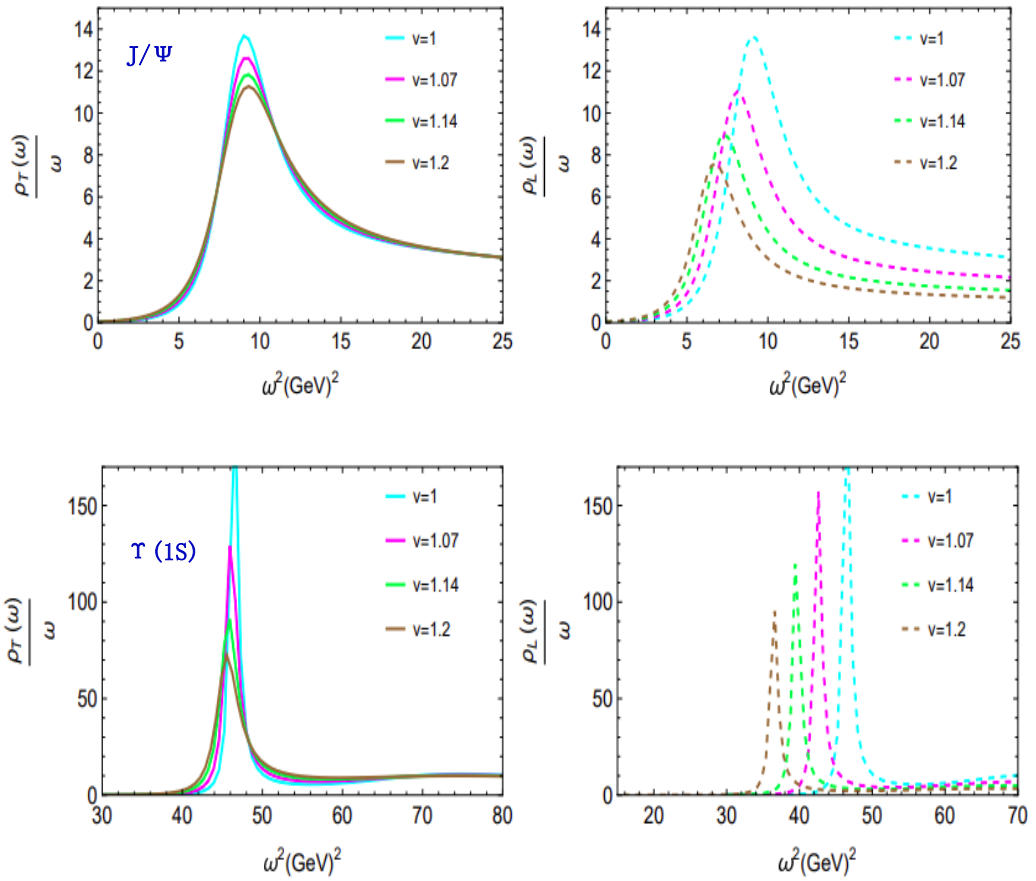
$$j^\mu = -\sqrt{-g} e^{-\phi(z)} F^{z\mu}.$$

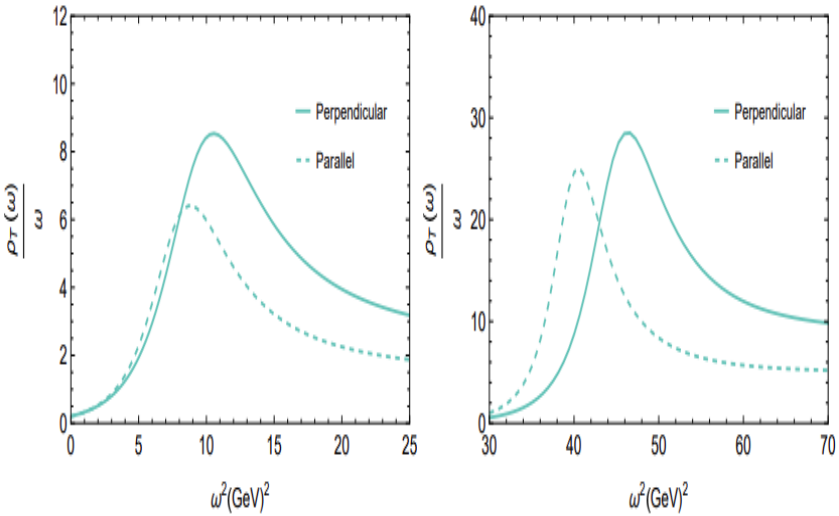
- The "conductivity" and its derivative are defined by

$$\sigma_L(\omega, \vec{p}, z) = \frac{j^{x_1}(\omega, \vec{p}, z)}{F_{x_1 t}(\omega, \vec{p}, z)},$$
$$\partial_z \sigma_L(\omega, \vec{p}, z) = \frac{\partial_z j^{x_1}}{F_{x_1 t}} - \frac{j^{x_1}}{F_{x_1 t}^2} \partial_z F_{x_1 t}.$$

Spectral functions of J/Ψ and ϒ(1S) with anisotropy

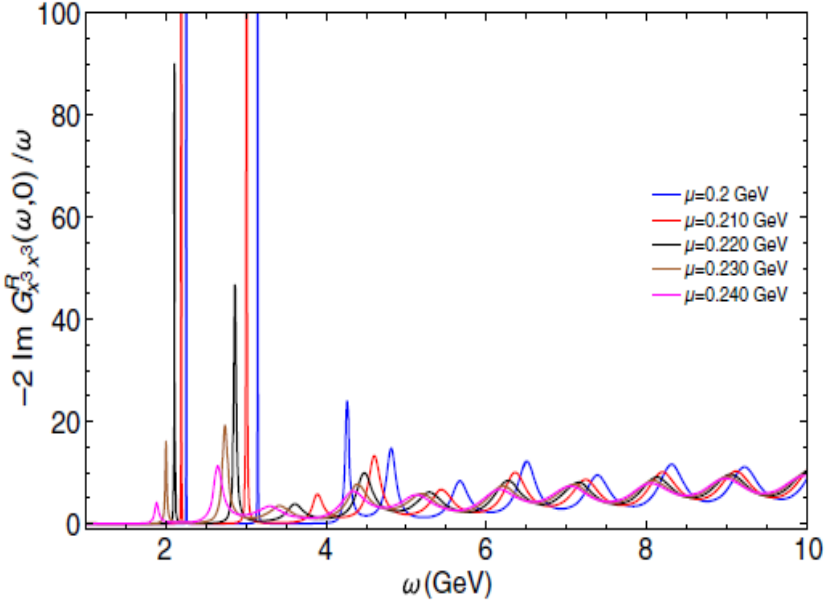
W.B. Chang and De-Fu Hou, Phys. Rev. D 109, 086010 (2024).

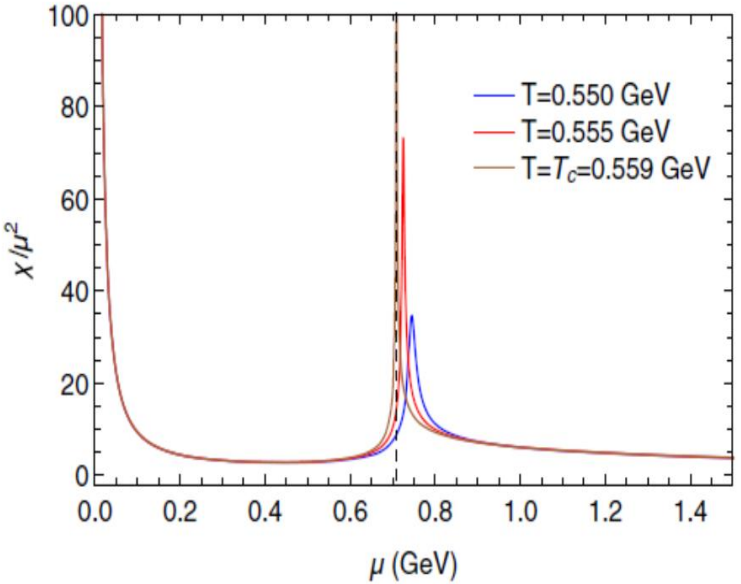




The spectral function of heavy vector mesons

Mamani, Hou, Braga, PRD 105, 126020 (2022)

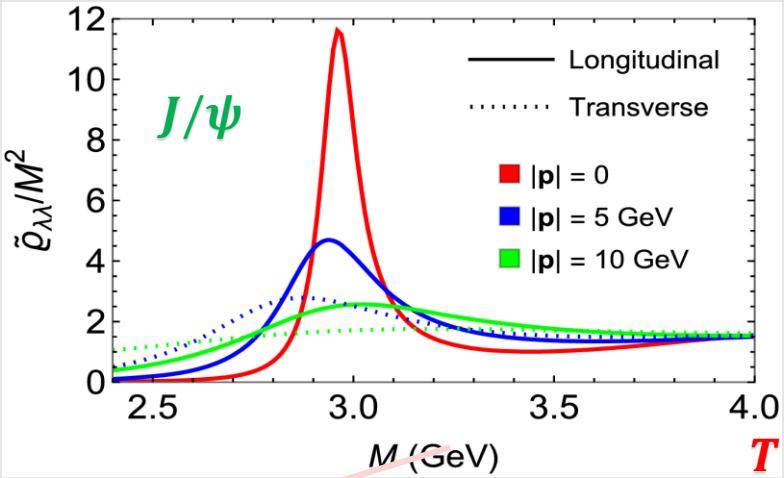




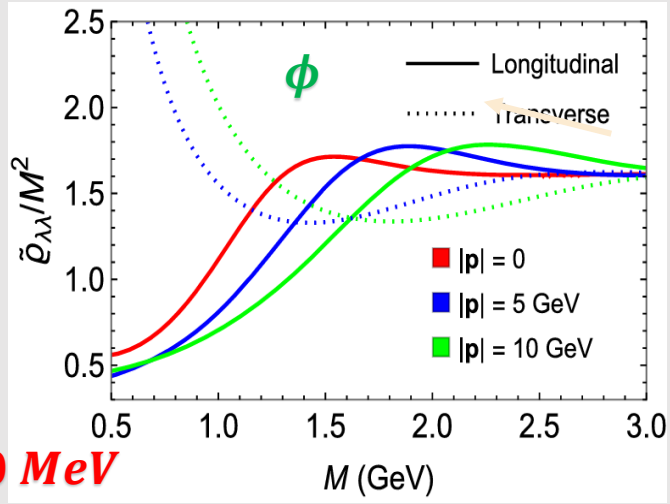
Spin alignments of J/ψ and ϕ mesons in hot plasma

Motion of J/ψ relative to a thermal background breaks symmetry between longitudinally polarized state and transversely polarized state

Spectral function



$T = 150\ MeV$

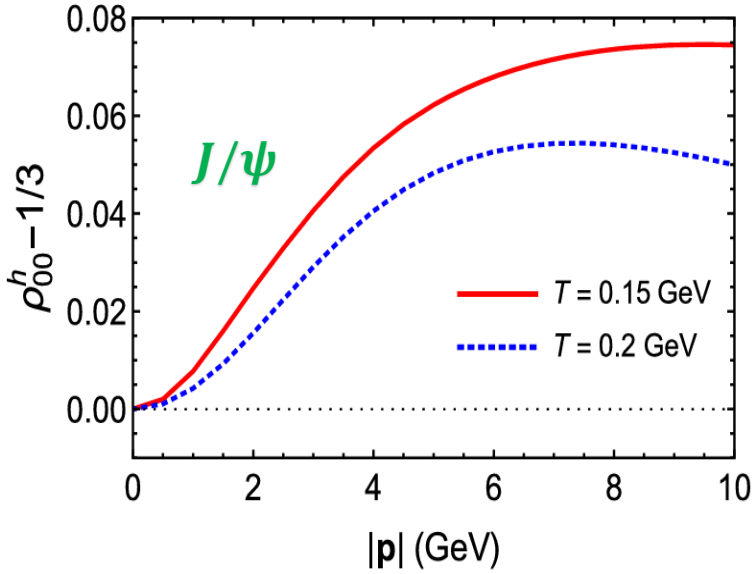


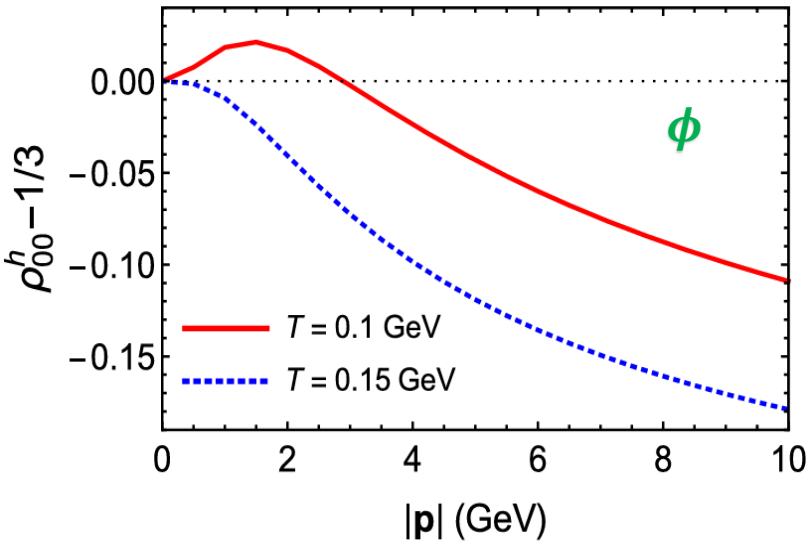
At zero momentum, spectral functions for all spin states are degenerate because of rotational symmetry.

XL Sheng,YQ Zhao SW Li , F Becattini, DF Hou PRD 110 (2024) 056047

Spin alignment in the helicity frame

XL Sheng,YQ Zhao SW Li , F Becattini, DF Hou PRD 110 (2024) 056047





A positive deviation from $1/3$, corresponding to a negative λ_θ parameter.

A negative deviation from $1/3$, absolute value becomes larger at larger $|p|$.

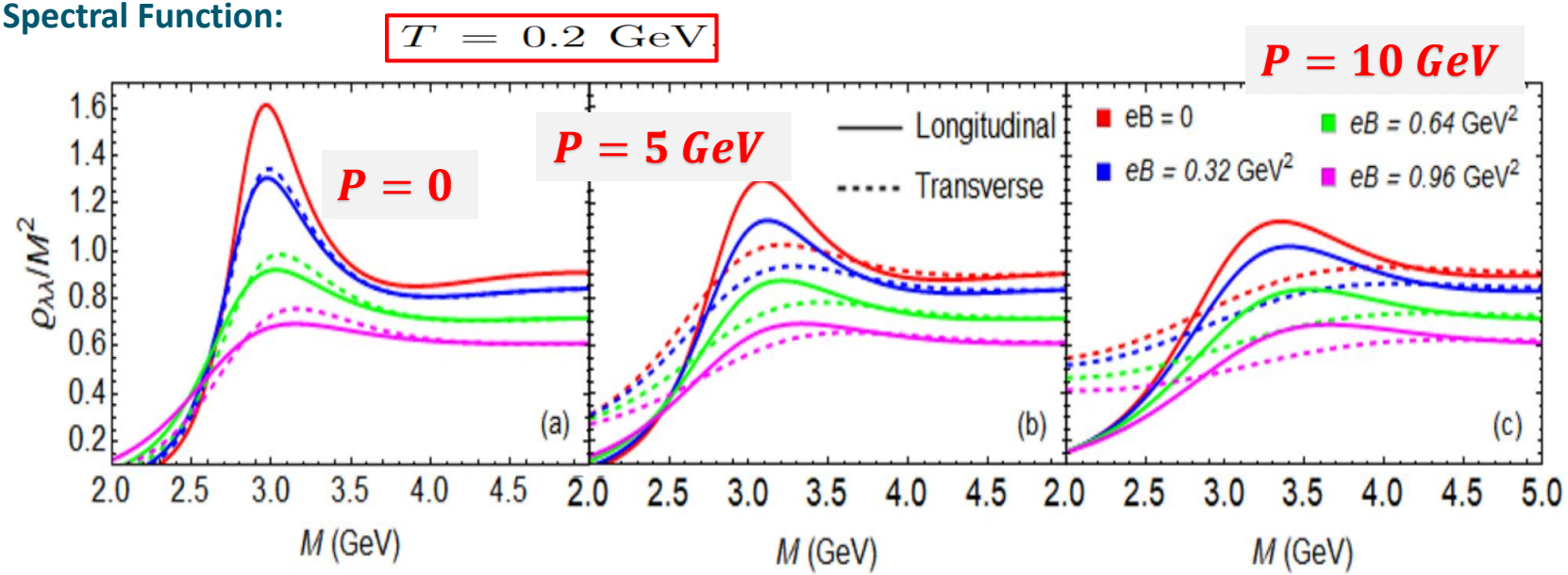
ρ_{00}^h at $T = 0.1$ GeV has a nonmonotonic dependence to $|p|$.

J/ψ meson in magnetized plasma

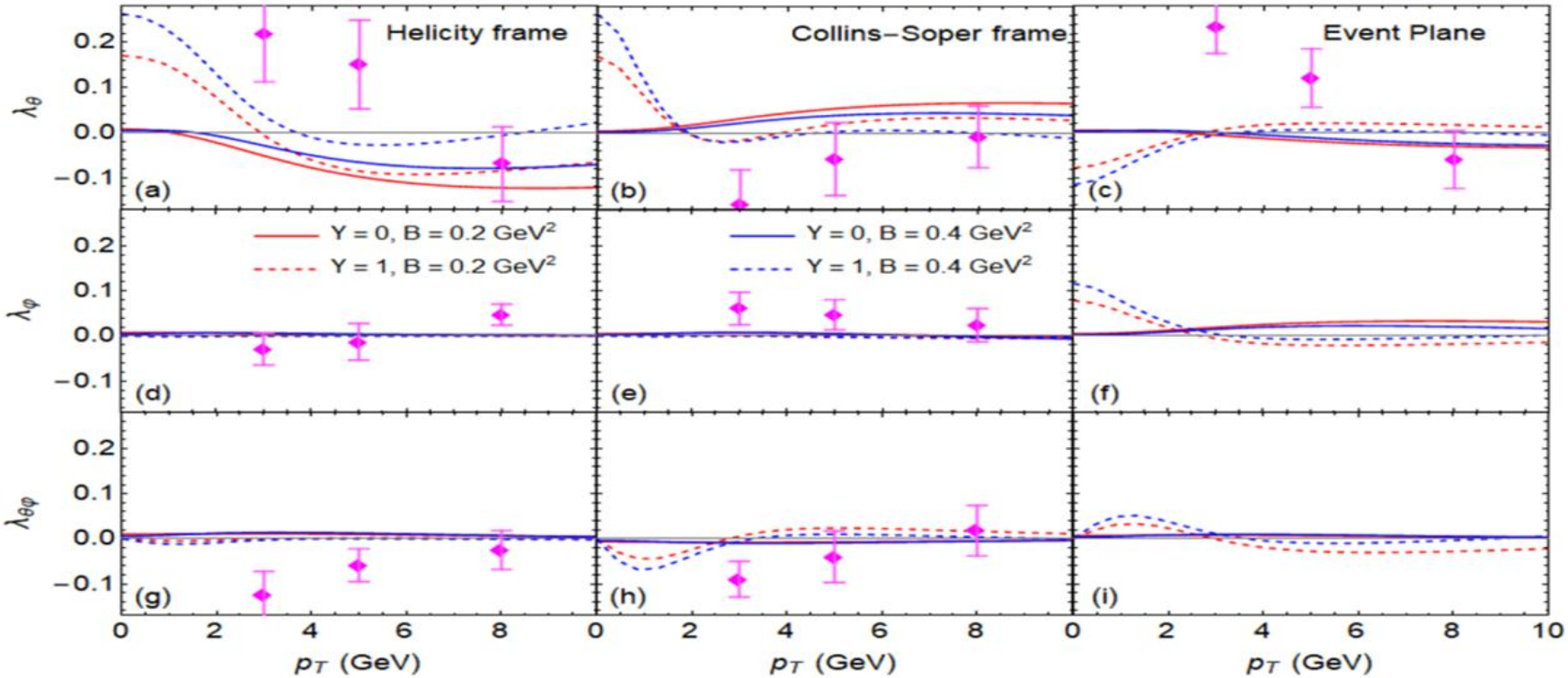
- Magnetic field parallel to momentum

Yan-Qing Zhao ,Xin-Li Sheng ,Si-Wen Li DF Hou , JHEP08 (2024)070

- Spectral Function:



A nonzero magnetic field or a nonzero momentum induces a separation between longitudinally and transversely polarized modes.



For the helicity frame and the Collins-Soper frame, we find that the λ_θ parameter is dominant when measuring along the event plane direction, all three parameters $\lambda_\theta^{\mathrm{EP}}$, $\lambda_\varphi^{\mathrm{EP}}$, and $\lambda_{\theta\varphi}^{\mathrm{EP}}$ are of the same order.

ALICE Collaboration, S. Acharya et al., Phys. Rev. Lett. 131 no. 4,(2023) 042303

Summary and outlook

Summary

• Holographic QCD (EMD/dilaton, soft-wall) captures the QCD phase diagram under magnetic field and rotation: inverse magnetic catalysis, CEP shifts, and transport near Tc

• Magnetic field and rotation reshape the phase diagram in opposite directions — μ promotes crossover→first-order; B promotes first-order→crossover

• Rotational effects: deconfinement T decreases with angular velocity, string tension enhanced (opposite to lattice, in line with most holographic results); chaos in dyonic black holes

• Spectral functions & spin alignment of heavy quarkonium: B and momentum split longitudinal/transverse modes; melting characterized via imaginary potential and thermal width

• Nucleon and pion structure from holography: mass spectra, electromagnetic & gravitational form factors, PDFs

Outlook

• How to introduce rotation more properly? (global vs. local, causality, horizon issues)

• Understand the tension between lattice and holographic results for rotational effects

• Explore finite density toward the CEP — testable in low-energy heavy-ion collisions and astrophysics.

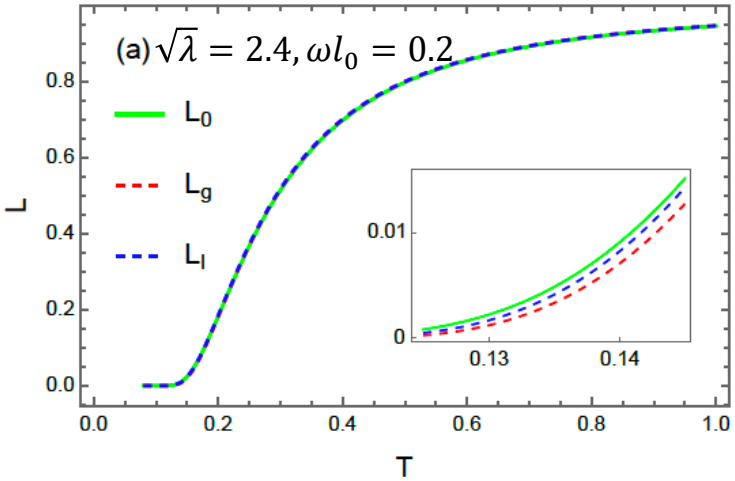
Thank you very much for your attention!

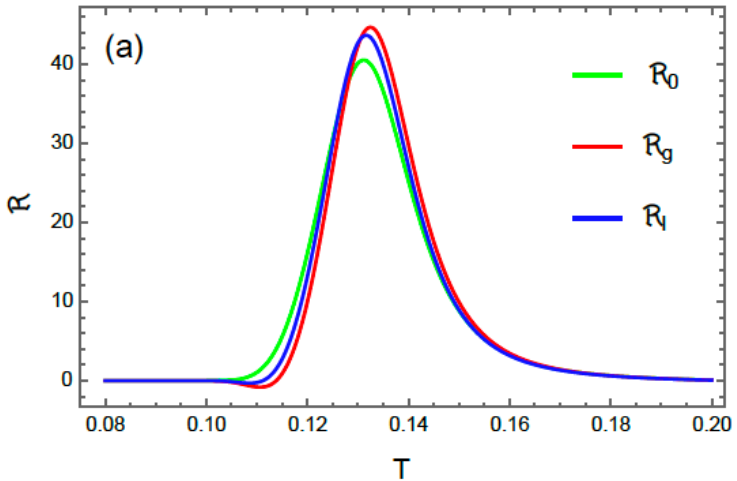
Deconfinement T

Jun-Xia Chen, Wang, Hou, Ren, Phys. Rev.D 110,026020 (2025)

$$L = L_0 + \omega^2 l_0^2 L_1$$

$$\mathcal{R} = \frac{|\frac{d^2L}{dT^2}|}{\left[1+\left(\frac{dL}{dT}\right)^2\right]^{\frac{3}{2}}} \simeq \mathcal{R}_0 + \omega^2 l_0^2 \mathcal{R}_1$$





Tc ↑

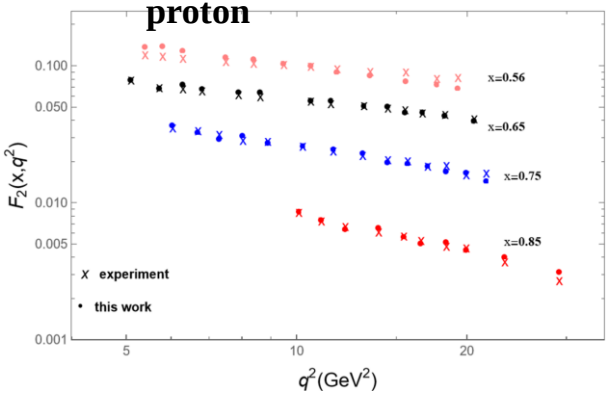
V. V. Braguta, A. Y. Kotov, D. D. Kuznedelev, et al, Phys.Rev. D 103 no. 9, (2021) 094515, arXiv:2102.05084 [hep-lat].

Nucleon structure from holographic QCD

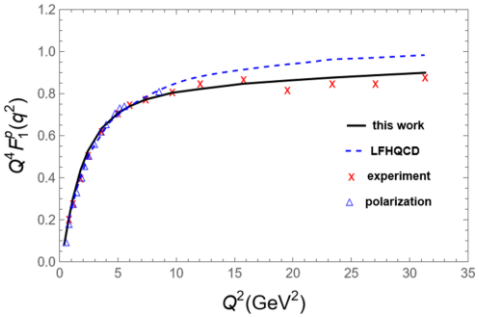
Mass spectrum of the proton

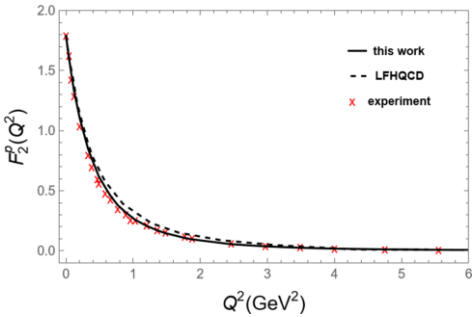
	proton	M_{exp}/Gev	other/Gev	Our/Gev	%M
n=1	N(939)	0.938	0.987	0.939	0.107
n=2	N(1440)	1.360 to 1.380	1.264	1.333	2.701
n=3	N(1710)	1.680 to 1.720	1.531	1.653	2.764
n=4	N(1880)	1.820 to 1.900	1.791	1.893	1.774
n=5	N(2100)	2.050 to 2.150	2.046	2.097	0.143
n=6	N(2300)	2.300	2.296	2.273	1.174

Structure functions of the proton

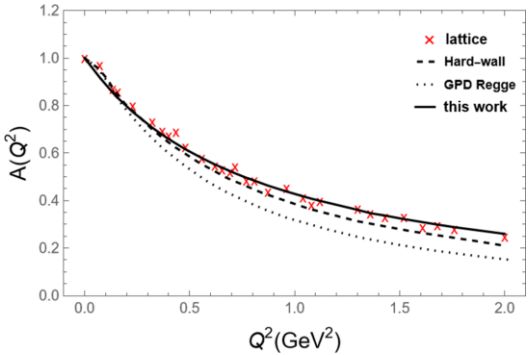


Electromagnetic form factor





Gravitational form factor



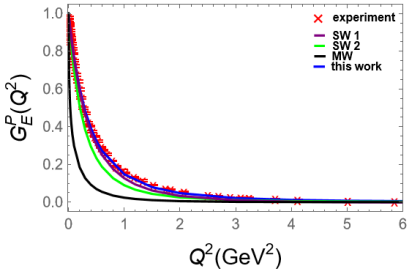
JL Deng , DF Hou , Phys.Rev.D 112 (2025) 3, 036011

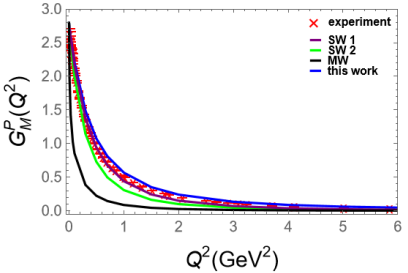
Nucleon structure from the holographic soft-wall model

Proton mass spectrum

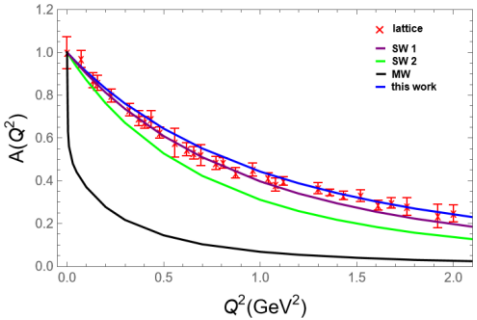
	Proton	M_{exp}/Gev	MW/Gev	SW 1/Gev	SW 2/Gev	Our/Gev	%M
n=1	N(939)	0.938	0.987	1.137	0.990	0.936	0.21
n=2	N(1440)	1.36 to 1.38	1.264	1.392	1.213	1.363	0.50
n=3	N(1710)	1.68 to 1.72	1.531	1.608	1.400	1.669	1.84
n=4	N(1880)	1.82 to 1.9	1.791	1.799	1.566	1.912	2.80
n=5	N(2100)	2.05 to 2.15	2.046	1.970	1.716	2.122	1.07
n=6	N(2300)	2.30	2.296	2.129	1.857	2.312	0.52

Electromagnetic form factor

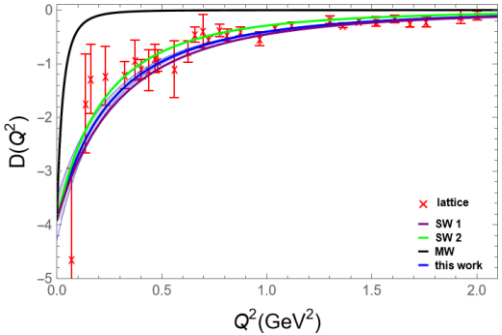




Gravitational form factor A



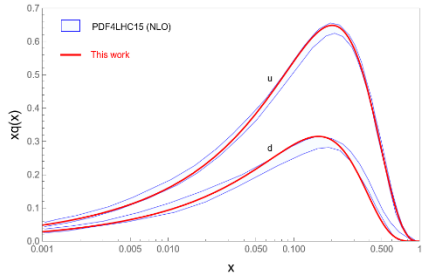
Gravitational form factor D



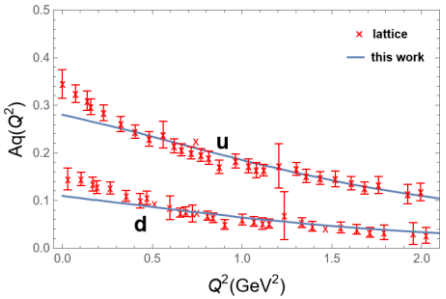
Jiali Deng and Defu Hou, Eur.Phys.J.C 86 (2026) 8, 947

Nucleon structure from light-front holographic QCD

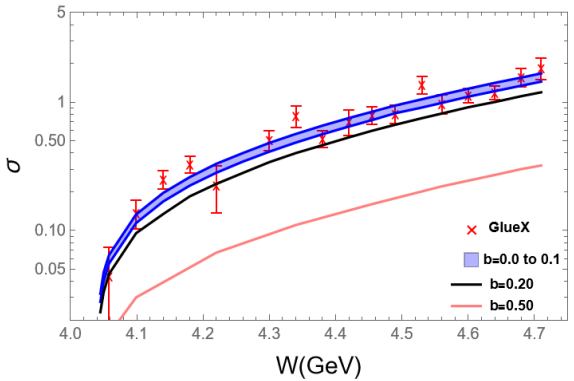
Quark PDF



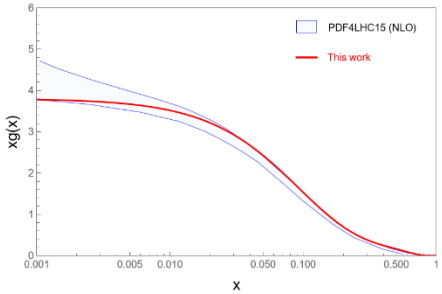
Quark GFF A



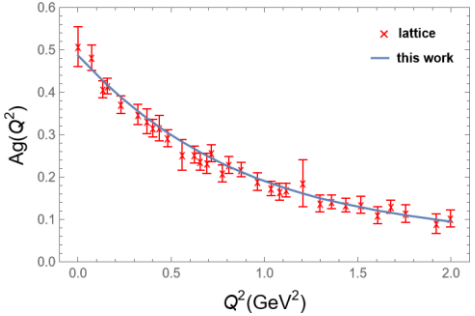
The total cross section σ(γp→J/ψp)



Gluon PDF



Gluon GFF A



b=0.04 ~~Trace~~ anomaly contribution 24%

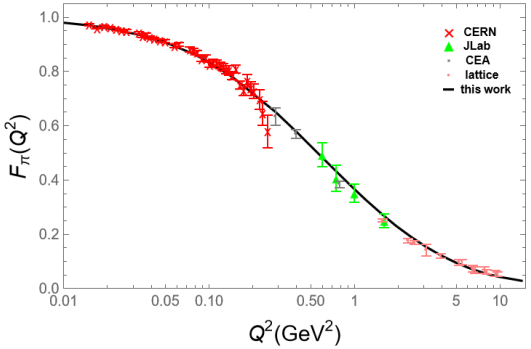
Jiali Deng and Defu Hou, Phys.Rev.D 114 (2026) 2, 026013

Pion structure from holographic QCD

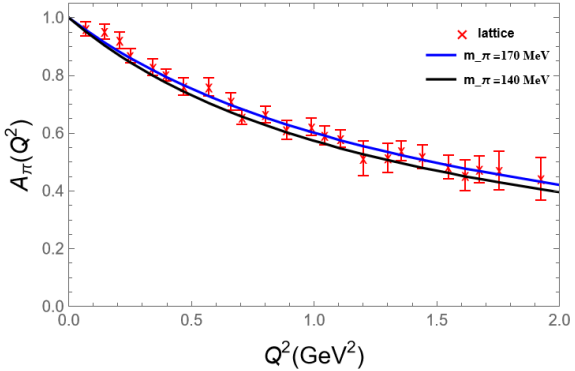
Pion mass spectrum

m_π	n=1	n=2	n=3	n=4	n=5
PDG(MeV)	139.6	1300±100	1812±12	2070±35	
Our(MeV)	139.6	1406	1892	2066	2278
Model 1(MeV)	140	1019	1793		
Model 2(MeV)	140	1520	2120		

Electromagnetic form factor



Gravitational form factor A



Jiali Deng and Defu Hou, Phys.Lett.B 880 (2026) 140866

Strong Coupling Expansion of Gluodynamics on a Lattice under Rotation

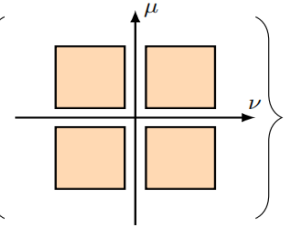
The action in the rotating background is[1]

$$S_G = \frac{2N_c}{g^2}\sum_X [(1-\rho^2\omega^2)\left(1-\frac{1}{N_c}\mathrm{ReTr}\bar{U}_{xy}\right)+(1-y^2\omega^2)\left(1-\frac{1}{N_c}\mathrm{ReTr}\bar{U}_{xz}\right)$$

$$+(1-x^2\omega^2)\left(1-\frac{1}{N_c}\mathrm{ReTr}\bar{U}_{yz}\right)+3-\frac{1}{N_c}\mathrm{ReTr}(\bar{U}_{xt}+\bar{U}_{yt}+\bar{U}_{zt})$$

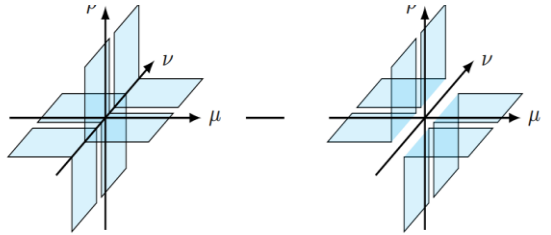
$$+\frac{1}{N_c}\mathrm{ReTr}\left(iy\omega\left(\bar{V}_{xyt}+\bar{V}_{xzt}\right)-ix\omega\left(\bar{V}_{yxt}+\bar{V}_{yzt}\right)+xy\omega^2\bar{V}_{xzy}\right)]$$

$$\bar{U}_{\mu\nu} = \frac{1}{4}\left\{\right.$$



$$\left.\right\}$$

$$\bar{V}_{\mu\nu\rho} = \frac{1}{8}\left\{\right.$$

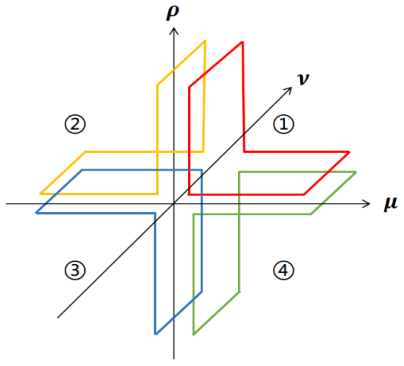


$$\left.\right\}$$

Spatial coordinate average $\sum_X \rightarrow \sum_P$ Plaquette average[2]

$$S_G = S_0 - \frac{1}{g^2}(E_0+\omega E_1+\omega^2 E_2)$$

$$\mathcal{Q} = \int \prod_{x,\mu} dU_\mu(x) e^{-S_G[U]}$$



[1] A. Yamamoto , Y. Hirono. PRL . arXiv:1303.6292.

[2] M. Gross, J. Bartholomew, and D. Hochberg. Report No. EFI- 83-35-CHICAGO, 1983.

FRGE study of the quark-meson model with ω and ρ vector mesons

- **A puzzling feature:** FRG studies often show a **back-bending** of the phase boundary at low temperature —an unphysical minus entropy.
- This behavior may result from pairing instabilities and insufficient regulation in IR.

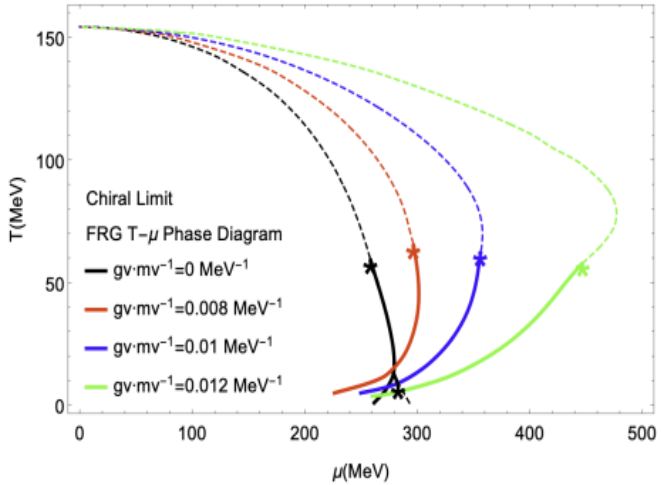


FIG. 2: The phase diagram of the FRG with different vector couplings. Dashed (solid) lines show the second (first) order phase transition. Stars show the tri-critical end point (TCP).

Zhang et al., Phys. Rev. D **96** *no.* 11 (2017)

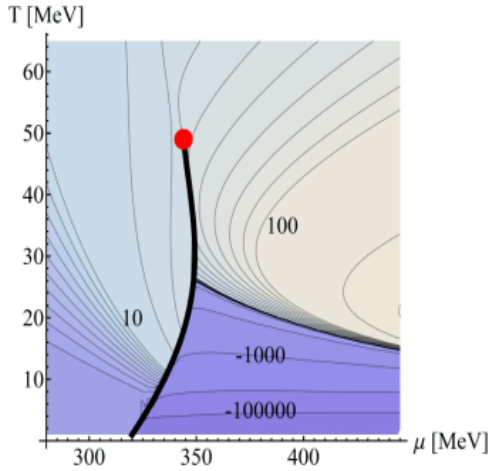


FIG. 4: (color online) The dimensionless entropy density, s/T^3, is shown as a contour plot together with the CEP and the first-order phase transition line, cf. Fig. 3. The inset numbers denote the corresponding values of s/T^3. Beyond the first-order line, a regime with negative entropy density is found.

Tripolt et al., Phys. Rev. D **97** *no.* 3 (201

Phase diagram @2+1 flavor

- Holographic model *with rotation*:
  - To introduce the rotation effect, we split the 3-dimensional space into two parts as $\mathcal{M}_3 = \mathbb{R} \times \Sigma_2$. Then the metric becomes to

$$ds^2 = -f(r)e^{-\eta(r)}dt^2 + \frac{dr^2}{f(r)} + r^2\ell^2 d\theta^2 + r^2 d\sigma^2$$

where $d\sigma^2$ denotes the line element of Σ_2.

  - We assume the system that has an angular velocity ω with a fixed radius ℓ, and consider the following local Lorentz boost

[5]. JHEP 07 (2021) 132 • e-Print: 2010.14478 [6].Phys.Rev.D 97 (2018) 2, 024034 • e-Print: 1707.03483
[7].JHEP 04 (2017) 092 • e-Print: 1702.02416 [8].Gen.Rel.Grav. 42 (2010) 1571-1583 • e-Print: 0911.2831

$$t \to \frac{1}{\sqrt{1-\omega^2\ell^2}}(\hat{t} + \omega\ell^2\hat{\theta}), \qquad \theta \to \frac{1}{\sqrt{1-\omega^2\ell^2}}(\hat{\theta} + \omega\hat{t}).$$

  - The corresponding metric can be written as

$$d\hat{s}^2 = g_{\mu\nu}d\hat{x}^\mu d\hat{x}^\nu = -N(r)d\hat{t}^2 + \frac{dr^2}{f(r)} + R(r)(d\hat{\theta} + Q(r)d\hat{t})^2 + r^2 d\sigma^2,$$

$$N(r) = \frac{r^2 f(r)\left(1-\omega^2\ell^2\right)}{r^2 e^{\eta(r)} - \omega^2\ell^2 f(r)},$$

$$R(r) = \frac{r^2\ell^2 - \omega^2\ell^4 f(r)e^{-\eta(r)}}{1-\omega^2\ell^2},$$

$$Q(r) = \frac{\omega\left(f(r) - r^2 e^{\eta(r)}\right)}{\omega^2\ell^2 f(r) - r^2 e^{\eta(r)}}.$$